Biocompatibility improvement of mesoporous silicon by PEGylation

Simo Näkki, 207435
Master's thesis
Physics degree
University of Eastern Finland
Department of Applied Physics
10th June 2013

University of Eastern Finland, Faculty of Science and Forestry
Physics degree, Medical physics
Simo Näkki: Biocompatibility improvement of mesoporous silicon by PEGylation
Master's thesis, 70 pages
Supervisors: Ph.D. Wujun Xu, Prof. Vesa-Pekka Lehto
June 2013

Keywords: Porous silicon, biocompatibility, biodegrability, PEG, drug delivery, colloidal stability

Porous silicon (PSi) has been extensively studied for its possibilities to be used in various applications. PSi has shown biocompatibility and biodegradability in addition to its many other properties such as tunable porosity and pore size. These properties have provoked numerous research groups across the globe to study and develop different applications for biomedical industry.

However aggregation of porous silicon nanoparticles and their fast clearance by RES (reticuloendothelial system) has restrained the use of porous silicon particles in intravenous applications such as therapy, diagnostics and drug delivery. In this thesis the manufacture of porous silicon and the surface modifications, that would provide proper properties for the material to be used in biomedical applications and specifically in intravenous dosing, are reviewed.

In the experimental section the porous silicon particles are PEGylated with three different sizes of PEG (polyethylene glycol) molecules and their long term stability is measured *in vitro*. Results indicate decreased aggregation and long term stability in measured time frame. The results also indicate dissolution of porous silicon particles in this time frame which is preferable when considering *in vivo* situation and applications in human body, where the dissolution of porous silicon to silicic acid and its excretion to urine is desired to achieve non-toxicity.

Abbreviations

ABC	Accelerated blood clearance
APTES	3-Aminopropyltriethoxysilane
BMD	Bone mass density
DSC	Differential scanning calorimetry
e^-	Electron
EPR	Enhanced permeability and retention
FTIR	Fourier transform infrared spectroscopy
h^+	Hole (empty electron state in valence band)
H_2O_2	Hydrogen peroxide
HF	Hydrofluoric acid
HLE	Human lens epithelial
HSR	Hypersensitivity reactions
IUPAC	International union of pure and applied chemistry
LDE	Laser Doppler electrophoresis
LDV	Laser Doppler velocimetry
MRI	Magnetic resonance imaging
PBS	Phosphate buffered saline
PEG	Polyethylene glycol
PNIPAM	Poly(N-isopropylacrylamide)
PSL	Porous silicon layer
PSi	Porous silicon
RES	Reticuloendothelial system
SBF	Simulated body fluid
SiF_6^{-2}	Silicon hexafluoride
Si-H_x	Silicon hydride
SiO_2	Silicon dioxide
TC	Thermally carbonized
TCPSi	Thermally carbonized porous silicon
TG	Thermogravimetry
TGA	Thermogravimetric analysis
THC	Thermally hydrocarbonized
THCPSi	Thermally hydrocarbonized porous silicon
TO	Thermally oxidized
TOPSi	Thermally oxidized porous silicon

Contents

1 Introduction

Arthur and Ingeborg Uhlir discovered porous silicon by accident in 1950s. They were making electropolishing experiments in aqueous HF-solutions and noticed that instead of being polished the surface had matte black, brown or red layer [1].

After its discovery, some investigations were done to study this phenomenon and theories about silicon dissolution were presented [2, 3]. However porous silicon did not obtain great interest until the work of Leigh Canham. First Canham discovered the photoluminescence [4] of porous silicon in 1990 and only five years later he reported the biocompatibility [5] of porous silicon. These studies done by Canham really triggered the wide scientific interest on porous silicon.

Nowadays there are multiple groups studying properties of porous silicon and its use in various applications, with many of them focusing on biomedical applications [6-10]. In biomedical applications mesoporous silicon is widely used because of its pore size. By definition of IUPAC (International Union of Pure and Applied Chemistry) the porous materials can be divided, according to their pore diameters, in three categories: microporous (< 2 nm), mesoporous (2-50 nm) and macroporous (> 50 nm).

The mesoporous material is most suitable for biomedical applications as the pores are big enough for effective loading, but also small enough to alter the properties of the loaded substance. Therefore the size of the pores play a crucial role in drug loading applications. The complete drug crystallization is prevented when pore sizes are only few times bigger than drug molecules [6, 7]. Also if the pores are too big, the drug can crystallize inside the pore and benefit of the loading is lost. The drug diffusion speed out of the pore is also proportional to the pore size.

Loading drugs into porous silicon has shown to improve the abilities of different drugs. It has been shown that loading modifies the dissolution rate of loaded drug [6]. It was found that the loading of poorly dissolving drugs improved dissolution whereas in case of highly dissolving drugs, a delayed release was seen. Loading has also been showed to increase the permeability of the drugs across cell membrane [11].

Previously meantioned properties suggest that porous silicon could be used in drug delivery applications as well as in imaging. The silicon particles are biocompatible and biodegradable which enables their use in intravenous dosing. With intravenous injections the particles could be used in imaging and therapeutic purposes, as particles

could circulate in blood and transfer the therapeutics in the desired location.

Silicon nanoparticles can accumulate in tumor tissues by EPR (enhanced permeability and retention) effect [12]. In normal tissue the epithelial is very tightly bounded but in tumor tissues the junctions are loosened, making the vasculature leaky. Now the nanoparticles can accumulate through these holes into the tumor and loaded therapeutics can effect on targeted area. This decreases the toxic effects elsewhere and gives best tumor control.

To ensure that therapeutics are not released while silicon nanoparticles are in blood circulation, the silicon particles can be coated with thermoresponsive polymers such as PNIPAM [13]. This polymer changes its composition when temperature is increased. At low temperatures PNIPAM is in extended form which prevents drug molecules from dissolving out of the pores. When temperature is increased, e.g. with ultrasonication, the PNIPAM degrades and drug molecules can dissolve out of the pores.

For imaging possibilities, the pores can be filled with iron oxide (Fe_3O_4) particles which are magnetic, and the particles can then be imaged with MRI (magnetic resonance imaging) [14]. However there are few critical factors restraining the possibility to use silicon particles for therapy and imaging. First thing is particle aggregation which increases the particle sizes rapidly in blood. As a result the particles are too big to circulate in small veins and get stuck e.g. in lungs or liver. Also RES (reticuloendothelial system) removes particles rapidly from blood circulation. The functioning of RES is based on adsorption of opsonin proteins on the surface of foreign particles and thus making them visible for macrophages which either destroy the particles by phagocytosis or transport them to RES organs (liver, spleen) for disintegration.

These two factors decrease blood circulation time of the particles to minutes which is not enough for any application. The blood circulation time should be at least 2-6 h for imaging applications and even several days for therapeutic applications to allow continous exposure on the target area [15]. PEG (polyethylene glycol) is hydrophilic, non-toxic and neutral molecule which has shown to decrease and prevent these adverse events and therefore increase the circulation time [16-22].

The PEGylation refers attaching PEG-molecules on the particle surface. Different PEG types and various attachment possibilities are dealt later on in this thesis. PEGylation is much studied and its benefits are well known. However only few studies regarding PEGylation have been done to porous silicon.

In this thesis the manufacture of porous silicon and its modifications towards biomed-

ical applications is reviewed. The focus is on the PEGylation of the porous silicon particles and its effect on the particle behavior. In the experimental section of this thesis the porous silicon particles are PEGylated by using three different PEG sizes (0.5 kDa, 2 kDa and 10 kDa). The long term stability for PEGylated particles is then evaluated. Finally, the possibility to attach molecules that are suitable for radiolabeling is studied. These molecules should not affect the stability of the PEGylated silicon particles and they should allow attachment of radioactive substances such as radioactive iodine ^{131}I so that particle circulation can be imaged in *in vivo* studies.

The aim of this thesis is to study the PEGylation phenomenon and the effect it has on the porous silicon particles. This thesis combines different results from various groups to find out the optimal method for PEGylation. The aim of the experimental work is to coat porous silicon particles with PEG molecules that would prevent particle aggregation and opsonin adsorption so the PEGylated PSi particles could be used in intravenous dosing.

2 Manufacture of Porous Silicon

Porous silicon can be fabricated in several different ways such as chemical stain etching [23], laser-induced etching [24] and anodic etching [1, 25]. More methods for fabrication of porous silicon can be found at comprehensive review done by Korotcenkov & Cho [26]. In this thesis our focus is on anodic etching because there are still problems on reproducibility, on attainment of porosity and thickness of formed layer with other methods available [26]. Therefore, anodic etching is still the most popular [26] method for silicon porosification and the mechanism of anodic etching is widely studied.

2.1 Anodic etching

Anodic etching, also known as electrochemical etching, is done in an etching cell where silicon wafer is used as an anode (Fig. 1). The cell is filled with chosen electrolyte which is usually hydrofluoric acid (HF) based. Surfactant, usually ethanol, is added to improve porosification. When current below certain threshold level is applied, silicon wafer starts to dissolve and porous structure forms to the surface of silicon wafer. If current above threshold level is used, the process is called electropolishing.

In electropolishing the surface of silicon wafer is smoothened and no porous silicon is formed. Etching can be done with controlling either anodic current or potential. Usually constant current is used as it gives better control for the porosity and thickness of the PSi layer [25, 27]. Also while using constant current the reproducibility is better from run to run [25, 27].

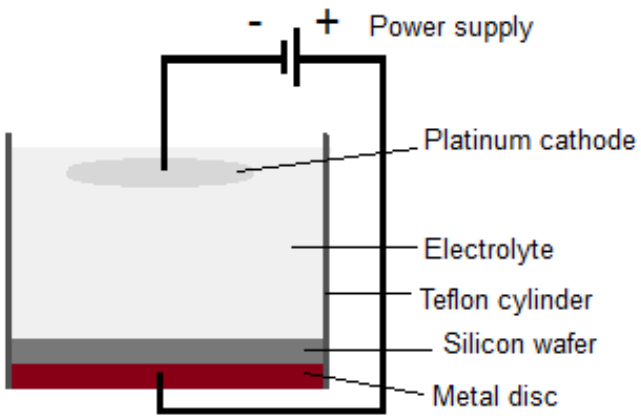

Figure 1: Standard etching cell used in manufacturing of porous silicon.

While the concept of threshold current is useful in determining current level for porosification, it still doesn't make clear limit for the process. Therefore concept of current density (J) is used. This way we can determine threshold for porosification which takes into account the different etching areas. Limit for porous silicon formation is now called electropolishing peak or porous silicon layer peak (J_{PSL}). Many factors affect the J_{PSL}-value, but usually porosification happens when current density from 1 to 100 mA/cm^2 is used [26].

The value of J_{PSL} can vary a lot, depending on the type and doping level of silicon wafers [25] and also the concentration of the used electrolyte [28]. Lehmann [29] has derived formula for the J_{PSL}-value.

$$J_{PSL} = C \cdot c^{1,5} \cdot e^{-\frac{E_a}{kT}}, \tag{1}$$

where the constant C is 3300 A/cm^2, c is the HF concentration, the activation energy E_a is 0.345 eV, k is the Boltzman constant and T is the temperature.

While we know PSi can be obtained by anodizing silicon wafer using current densities under the J_{PSL}-value, there are still many factors effecting on the properties of the forming PSi layer. These factors include the electrolyte concentration and composition, current density, temperature, etching time, possible illumination and the properties of used silicon wafer such as doping level, wafer type and crystalline orientation, etc. [25, 27, 30]. Let us briefly consider the effect of few parameters to the properties of porous silicon layer.

As already seen on equation (1) the rise of HF concentration increases the J_{PSL}-value and thereby affects the current values that can be used in porosification. It could be assumed that HF-concentration would thereby also affect the properties of PSi. When anodizing silicon wafer, and the other parameters are constant, a decrease in porosity [25] and pore diameter [31] can be seen as the HF concentration increases (Fig. 2). HF concentration also affects the depth of the pores [31] which increase with increasing concentration.

Another parameter that has a great effect on PSi properties, is current density. While current density is increased the porosity also increases when using p-type wafers (Fig. 2b) [25, 30]. As already mentioned the type of silicon wafer affects the forming PSi layer properties. When n-Si wafers were used porosity behaves quite differently compared to p-type (Fig. 3a) [25, 30, 32].

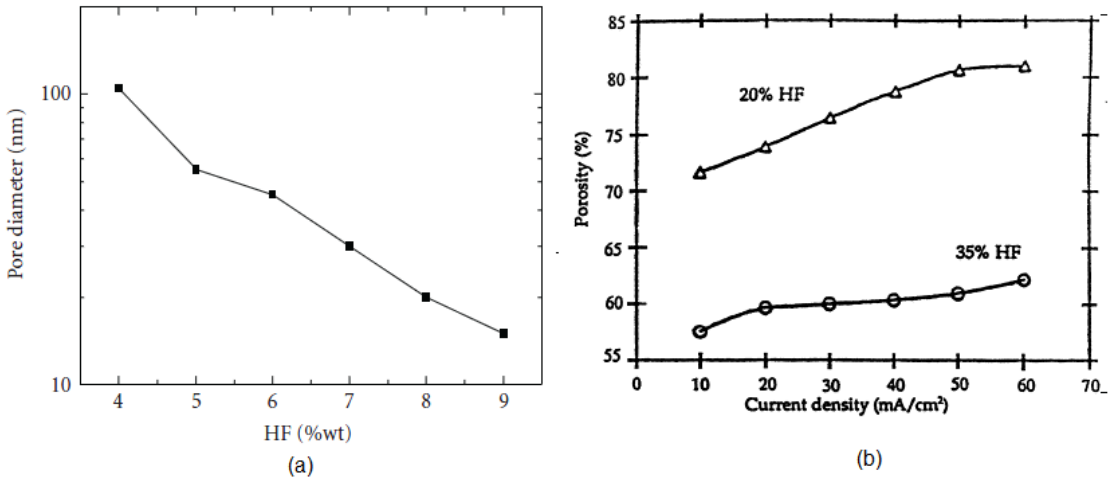

Figure 2: The effect of HF concentration on (a) pore size on n-Si [31] (b) porosity and the effect of current density on porosity on p-Si [25].

Below certain current density the porosity of n-type PSi decreases even though current density is increased. However after certain J value the n^+-Si behaves as p-Si (Fig. 2b) [25]. Current density also affects the pore size. On the study done by Rumpf et al. [33] an increase in porosity and pore diameter was seen when current density was increased. As other parameters increase it is logical that pore-distance will decrease (Fig. 3b).

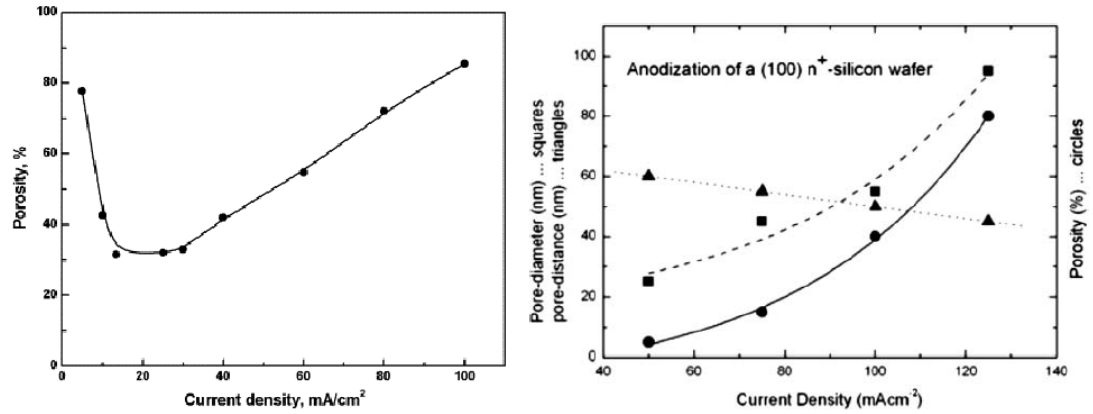

Figure 3: The effect of current density on (a) porosity on n-Si [32] (b) porosity, pore size and pore-distance on n^+-Si [33].

As illustrated in Fig. 2 and Fig. 3a change of few parameters on etching can have drastic effect on forming PSi layer. We won't go any further into details on the effect of other parameters here but as clarification some of the effects on porous silicon can be seen from Table 1 [30, 34].

Table 1: Summary of few parameters affecting on porous silicon layer

	Parameters	
An increase of	Porosity	Pore diameter
HF concentration	Decreases	Decreases
Current density	Increases	Increases
Doping (p-type)	Decreases	Increases
Doping (n-type)	Increases	Decreases

As we can see from Table 1 the precise control of all parameters is essential for high quality porous material which is suitable for the desired application. Usually parameters we want to tune are (as in Table 1) porosity and pore diameter. At the end of etching a short current pulse is given for detaching the PSi layer from the silicon substrate. The current density of the end pulse must be higher than the J_{PSL}-value. The detached porous layer can be scraped off from bulk silicon with scalpel.

After etching, the pores of PSi films are filled with electrolyte which must be removed. Different ways have been developed for drying the PSi films [35], but the easiest way for most films is to use oven for vaporizing electrolyte out of the pores. In practice films aren't useful and, therefore they must be milled into particles. Milling can be done by e.g. a ball mill. With milling time and ball size the particle size can be controlled depending on application, e.g. in medical applications nanoparticles are mostly used.

After etching there are dangling bonds of Si which are submissive for forming bonds with hydrogen. It has been confirmed that after etching the surface is covered with Si-H_x compounds [27, 36], where x can be from 1 to 3. Bonds between Si and H_x are not stable [36] and so PSi surface is susceptible for impurity attachments, from which oxygen is the most common [27]. This "ageing" is unwanted and thereby we want to store the material as well as possible and also stabilize the surface so it won't react with impurities. Stabilizing can be done in many different ways [27, 36] which we will deal with later on but let's first go through the mechanism of porosification.

2.2 Mechanism of porous silicon preparation

Porous silicon is quite easy to produce with etching set up shown in Fig. 1, but the mechanism or theories about it are entirely something else. Although porosification is known for over 50 years, the mechanism behind the process is poorly understood and many different models have been proposed. Some factors are widely accepted even though mechanism behind them is unclear: holes are crucial for the dissolution and the bottom of the pores is favored path for the electrochemical current and thereby the site for dissolution [26, 37]. Let's view next two existing theories that explain porous silicon dissolution without going too deep into details.

Turner [2] and Memming & Schwandt [3] have suggested following overall reaction for the dissolution of porous silicon in fluoride media

$$\begin{aligned} \mathrm{Si} + 2\,\mathrm{HF} + \lambda \mathrm{h}^+ &\rightarrow \mathrm{SiF_2} + 2\,\mathrm{H}^+ + (2-\lambda)\mathrm{e}^- \\ \mathrm{SiF_2} + 2\,\mathrm{HF} &\rightarrow \mathrm{SiF_4} + \mathrm{H_2} \\ \mathrm{SiF_4} + 2\,\mathrm{HF} &\rightarrow \mathrm{H_2SiF_6}, \end{aligned} \tag{2}$$

where h^+ indicates holes (empty spaces in valence band), e^- indicates electrons and λ is the number of charges exchanged. The net reaction for dissolution of silicon can be also written in form [38]

$$\mathrm{Si} + 6\,\mathrm{HF} + \mathrm{h}^+ \rightarrow \mathrm{SiF_6^{2-}} + 4\,\mathrm{H}^+ + \mathrm{H_2} + \mathrm{e}^-. \tag{3}$$

Reaction (3) describes dissolution of silicon under most commonly studied conditions [38]. As can be seen from the equations (2) and (3), holes are crucial for the dissolution of silicon. In p-type silicon wafer holes are present, but in n-type they need to be produced. This can be done e.g. by illumination. If illumination is low, there appears a competitive reaction on n-type silicon [38]

$$\mathrm{Si} + 6\,\mathrm{HF} + \mathrm{h}^+ \rightarrow \mathrm{SiF_6^{2-}} + 6\,\mathrm{H}^+ + 3\,\mathrm{e}^-. \tag{4}$$

While Si-wafer is in HF, the surface is covered with hydrogen which makes it inactive to dissolution. When voltage is applied the holes are generated and shifted to the silicon-electrolyte surface. At the surface, holes remove Si bonds and make Si atoms

sensitive for interactions with the electrolyte. Thereby at the end, silicon atom can be dissolved into the electrolyte and pores can be formed [26].

Formed pores can have different morphologies depending on etching conditions. Micropores usually have sponge-like morphology and mesopores tend to form perpendicular to the surface with side pores (Fig. 4) [26].

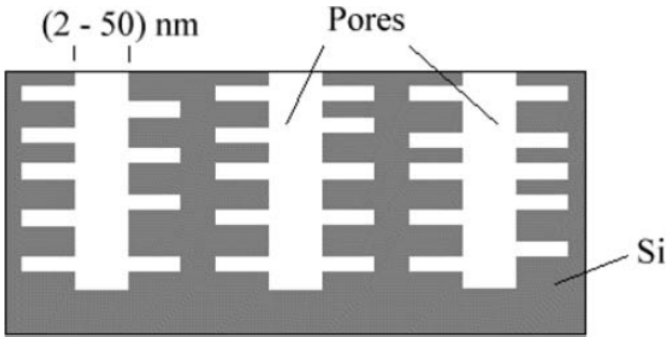

Figure 4: Schematic picture of mesoporous layer formed on etching [26].

Another, and more comprehensive, theory for porous silicon formation is called Gerischer mechanism or Gerischer mechanism revisited (Fig. 5) [38]. In Fig. 5 there are seven steps (1-7) and step (5) is divided in two parts. Of these, the first part (5a) is called current doubling and second part (5b) is called current quadrupling. These routes correspond to the equations (3) and (4), respectively [38].

In first step (1) a hole is generated in to bulk silicon (e.g. by voltage) and in step (2) the hole has shifted to the surface by the effect of the anodic bias. In step (3) hydrogen (H) atom is substituted with fluorine (F^-) atom by the effect of the hole arriving to the surface. Attached fluorine polarizes silicon backbonds which makes the Si atom susceptible for more fluorine attachment (step (4)) [38, 39].

As mentioned earlier the step (5) is divided in two parts. Step (5a) is commonly observed: $SiHF_2$ reacts with either HF^-, HF or H_2O and the silicon atom is released from the bulk material. Let's here just consider reactions with the HF-species as they are

$$SiHF_2 + HF_2^- \rightarrow SiHF_3 + F^-, \quad (5)$$

$$SiHF_2 + HF \rightarrow SiHF_3. \quad (6)$$

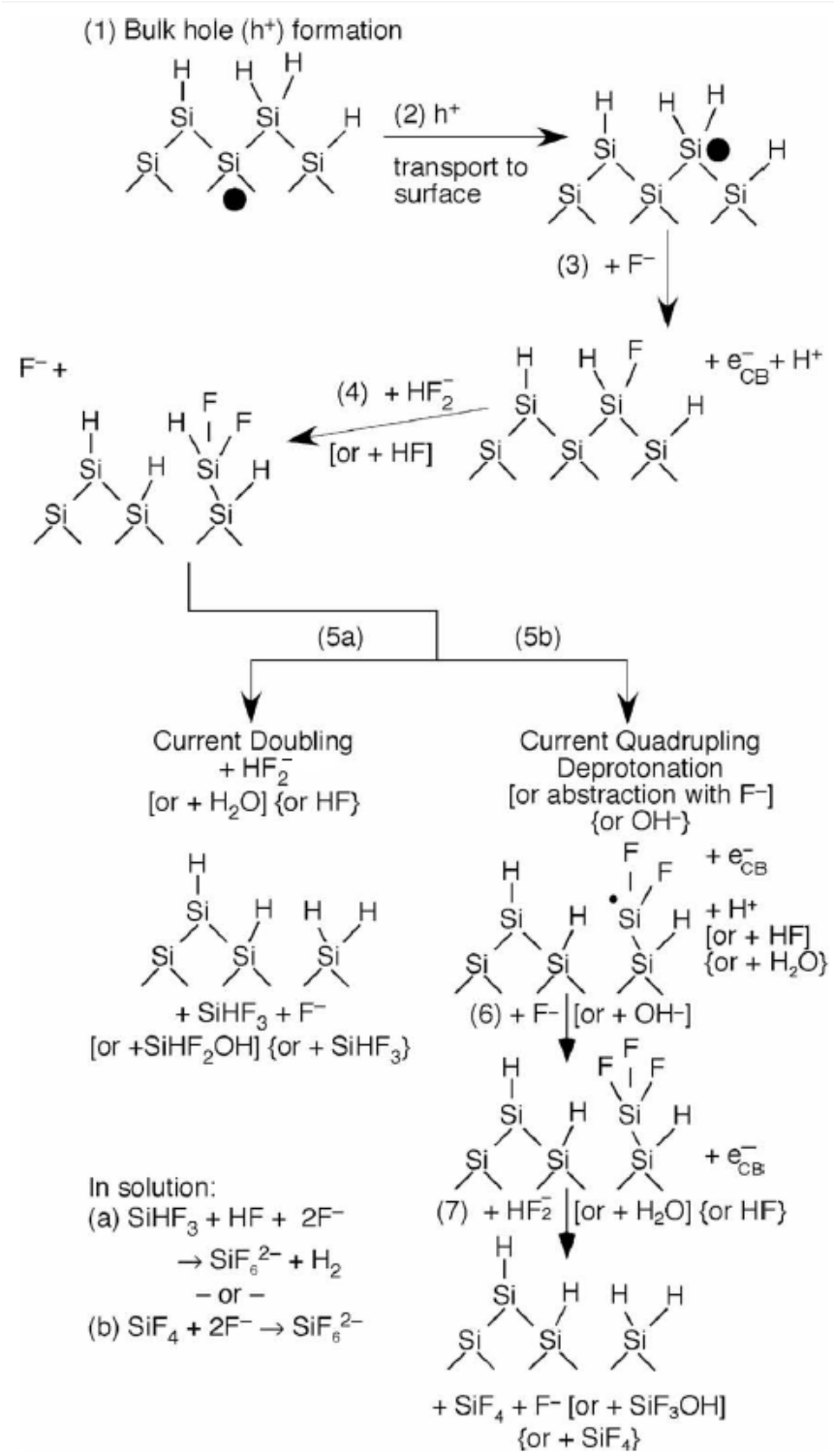

Figure 5: The Gerischer mechanism modified by Kolasinski [39] and contributions from Kooij and Vanmaekelbergh [40]. [38] Alternative reactants for a given step are in brackets.

Final reaction happens rapidly in liquid, forming the final product

$$\mathrm{SiHF_3 + HF + 2\,F^- \rightarrow SiF_6^{2-} + H_2}. \tag{7}$$

The competitive reaction (5b), which occurs on low illumination on n-type, starts with deprotonation or abstraction according to next reactions (reaction with $\mathrm{OH^-}$ is ignored here)

$$\mathrm{SiHF_2} \rightarrow \quad {}^{\bullet}\mathrm{SiF_2 + H^+} \qquad \text{deprotonation,} \tag{8}$$

$$\mathrm{SiHF_2 + F^-} \rightarrow \quad {}^{\bullet}\mathrm{SiF_2 + HF} \qquad \text{abstraction.} \tag{9}$$

In step (6) fluorine $\mathrm{F^-}$ is attached to the dangling bond. Step (7) is very similar to step (5a) as reactions occur with either HF or $\mathrm{HF_2^-}$ and silicon atom is dissolved.

$$\mathrm{SiF_3 + HF_2^-} \rightarrow \mathrm{SiF_4 + F^-}, \tag{10}$$

$$\mathrm{SiF_3 + HF} \rightarrow \mathrm{SiF_4}. \tag{11}$$

Final reaction occurs again in liquid as final product is formed without nitrogen gas evolution [38]

$$\mathrm{SiF_4 + 2\,F^- \rightarrow SiF_6^{2-}}. \tag{12}$$

While many theories are proposed [26, 37, 38, 41], the mechanism behind porosification still remains unclear. One essential fact that still remains a mystery, is theory about pore initiation. While many theories give reasonable good explanations for dissolution, the theories about pore initiation haven't found mutual language between them. Currently pore initiation has been proposed to start on e.g. structural defects or micro-cavities [26].

2.3 Surface modifications

As mentioned earlier at the end of chapter 2.1, modification of the fresh PSi surface is needed. Surface can be stabilized e.g. by oxidation or thermal carbonization [27]. In thermal carbonization dried PSi sample is heated in the oven in the presence of acetylene gas (C_2H_2). Acetylene is a gas that adsorbs on the surface of PSi already at room temperature. As temperature is increased above 400 °C the acetylene starts to dissociate. Simultaneously hydrogen starts to desorb from the PSi surface and carbon atoms are bound to the surface [27].

As different temperatures are used two different surface terminations can be achieved. When temperatures are below 700 °C the formed surface is containing hydrocarbons and material is called thermally hydrocarbonized porous silicon (THCPSi). When increasing the temperature, all hydrogen will desorb out from the surface and surface will be covered only with carbon atoms and material is referred as thermally carbonized porous silicon (TCPSi) [27].

So by adjusting temperature, two different kinds of surface modifications can be done. Both surfaces are stable but the difference now is that the surface modified with lower temperatures (THCPSi) is hydrophobic whereas TCPSi surface is hydrophilic [27].

Another great, and simple, way to stabilize the surface is to oxidize it. This can be done e.g. thermally or chemically [27, 36]. When porous silicon is heated in air (300 °C) the surface will be partially oxidized. Oxygen atoms will attack the surface silicon atom back-bonds and form oxygen bridge between surface silicon atoms and the silicon atom layer underneath [27]. When temperature is raised also the Si-H interface is modified as oxygen penetrates between Si-H bonds [42] (Fig. 6). Still minor oxidation in between Si and H atoms can already occur in 300 °C. After the oxidation the PSi surface is hydrophilic and the material is referred as TOPSi (thermally oxidized porous silicon). The hydrophilic nature of particles is desired for many drug delivery applications [27].

In chemical oxidization the amount of Si-H groups is reduced by oxidizing them as Si-OH groups [43]. This way surface is covered mostly with hydroxyl groups which is favored for many molecular binding reactions. Some frequently used chemicals are mixtures of hydrogen peroxide (H_2O_2), ammonium hydroxide (NH_4OH) and water and hydrogen peroxide (H_2O_2), hydrochloric acid (HCl) and water [43, 44]. We denote this material, first thermally oxidized and subsequently chemically oxidized, as TOPSi-OH.

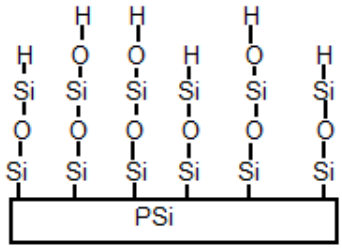

Figure 6: Schematic picture of the porous silicon surface after thermal oxidation

Finally the stabilized porous silicon particles are functionalized with suitable molecules. For bioapplications this means usually molecules that enable specific and targeted drug delivery. Surface can be modified with e.g. DNA [45] or proteins [46]. However maybe the most frequently attached molecules are amine-groups [43, 47-49] and polyethylene glycol (PEG) [20, 44, 48, 50-54].

Amine groups can be quite easily covalently bonded to the oxidized (TOPSi-OH) porous silicon by silanization [43, 49]. In this process APTES (3-aminopropyltriethoxysilane) (Fig. 7) is used. The surface of amine-group (NH_2) grafted porous silicon becomes more positive [43] and it also makes surface more reactive towards biomolecules as molecules can now be attached to the amine group [43, 47, 48].

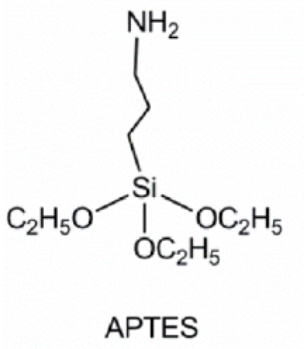

Figure 7: Structure of APTES. [43]

Other frequently used molecule is polyethylene glycol (PEG) which is used in many applications, e.g. in health and beauty aids. PEG is a biomolecule that has repeating ethylene ether unit structure (n number of ethylene ether units) (Fig. 8). Usually there are two different parts, in addition to actual PEG: end that attaches to porous silicon (determined R_1) and distal part that interacts with solvent (R_2) [15].

There are currently different kinds of PEG's available: linear PEG (Fig. 8b), branched PEG, star PEG and comb PEG [15]. Here we will focus on linear PEG and its usage

Figure 8: Basic structure of PEG. (a) Ethylene glycol. (b) PEG with n ethylene units and distal ends R_1 and R_2. [15]

in surface modifications. There are many different sizes of linear PEGs as the size increases with the number of ethylene ether units (n) in PEG. Usually these PEGs are classified by the molecular weight (M_w) such as 500 Da, 2000 Da and 20000 Da PEG. The weight of ethylene glycol, one monomer in PEG, is about 44 Da and length is 3,5 Å[15]. This means that e.g. 2000 Da PEG has about 46 ethylene glycol units and the length is 15,8 nm.

The distal ends of PEG (R_1 & R_2) are crucial as they determine whether or how PEG can be attached to PSi particles and how the particles interact in solvents. R_2 is usually chosen as hydroxyl or methoxy group as they prevent protein adsorption [21, 50, 51]. One possibility is to attach targeting molecules, such as antibodies [55, 56, 57] or radiolabeled peptides [58] that also enables radio imaging, to the distal end (R_2).

There are many ways to attach PEG to the surface [53] and it can be done by e.g. bonding PEG covalently to already bonded molecule [20, 52] or by using silanization [19, 44, 53] (Fig. 9). The process where PEG-molecules are attached to the surface of particle, no matter what way, is referred as PEGylation.

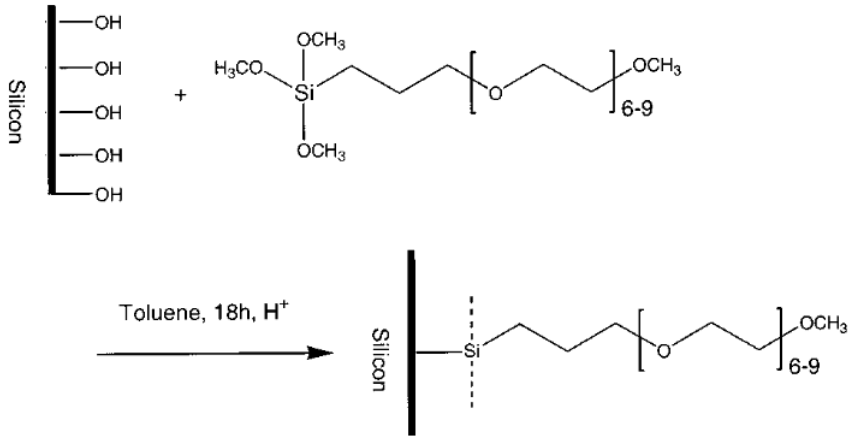

Figure 9: Scheme for covanlent bonding of PEG by silanization. [53]

3 Properties of porous silicon

Porous silicon has many unique properties that are utilized in various applications. These properties include tunable pore size and porosity, large effective pore volume and pore area, changed electrical and thermal conductivity compared to bulk silicon and much more [26]. However the most interesting properties of porous silicon are its photoluminescent properties [4] and the fact porous silicon is biocompatible [5]. Here we discuss biocompatibility in more detail and aspects related to it.

3.1 Biocompatibility

The term biocompatibility is a essential word for distinguishing biomaterial from other materials [59]. Biomaterial science uses the term biocompatibility frequently but its actual meaning is not clear. Originally biocompatibility was meant for describing abilities of implantable devices that would stay longer times on patient. However with new degradable devices the original definition was modified and stated as

Biocompatibility refers to the ability of a material to perform with an appropriate host response in a specific situation. [60]

However this definition still doesn't clarify or specify what biocompatibility means and therefore more describing definitions have been proposed:

Biocompatibility refers to the ability of a biomaterial to perform its desired function with respect to a medical therapy, without eliciting any undesirable local or systemic effects in the recipient or beneficiary of that therapy, but generating the most appropriate beneficial cellular or tissue response in that specific situation, and optimising the clinically relevant performance of that therapy. [61]

This definition is more appropriate and comprehensive. This definition also includes materials that can be e.g. injected or orally dosed to the human body. Biocompatibility can by this definition include lots of different properties which vary depending on the application.

Porous silicon has been shown to be bioactive and biodegradable [5] which are properties of PSi that states it as biocompatible material. Pore size and porosity affect much on these properties as highly porous (p >70 %) PSi dissolves quickly in SBF (simulated body fluid) but when porosity degreases under 70 % the material becomes bioactive and slowly biodegradable. If porosity decreases low enough, the material

properties are similar to bulk silicon and material is bioinert. Also, the material becomes bioinert if the pore size increases above 50 nm (macroporous PSi) [27]. This way by tuning porosity and pore size the properties can be influenced.

Bioactivity has been shown by growing hydroxyapatite [5, 62], a form of calcium phosphate that comprises the mineral phase of bone [59], to the surface of PSi. Also other cells such as human ocular cells (human lens epithelial, HLE) has been successfully grown to the surface of PSi [63]. Because of bioactive properties, porous silicon could be exploited e.g. in bone implants.

Porous silicon has also found to be biodegrable [5]. Porous silicon is shown to dissolve in simulated body fluids (SBF) forming monomeric silicic acid ($Si(OH)_4$) by reactions showed below [10, 27]

$$Si + 2O \rightarrow SiO_2 \tag{13}$$

$$SiO_2 + 2H_2O \rightarrow Si(OH)_4. \tag{14}$$

The dissolution is affected by manufacturing conditions and surface modifications and can vary from just few hours to several months [63]. The amount of silicic acid can be controlled with porosity; higher the porosity faster the dissolution and more silicic acid is formed. Temperature and pH also affects the dissolution of silicon as degradation increases with increasing temperature and pH [64].

Main thing about silicon dissolution is its non-toxicity (very low toxicity), e.g. mammalian cells grown into porous silicon wafers remained viable and no toxic effects were seen [65]. The average western people get daily intake 20-50 mg of Si from normal groceries, e.g. especially beer is major source to the Si intake [66]. The intaken silicon is then dissolved as silicic acid, which is most natural form of silicon in nature [27], according the reactions above. Body can handle small amounts of silicic acid efficiently by urine excretion [27] so small amounts are not dangerous for humans.

In contrast to the ability of body to handle silicic acid there have also been studies how Si intake effects BMD (bone mass density). It has been reported that silicon intake has had positive effect on BMD as it seems that silicic acid is actually important for optimal bone and collagen growth [64, 66].

Listed properties (biodegradability and bioactivity) speak for biocompatibility of silicon but there are still few important facts to consider. First one is the colloidal stability of the particles and second is the respond to the cells in blood. When think-

ing applications where porous silicon nanoparticles are injected to the blood it is important that they stay as separate particles and that they would circulate in the blood long enough to carry out their intended function.

Size of the nanoparticles is one of the most important issues when thinking intravenous drug delivery, therapy and imaging. The human body (blood veins) and immune system efficiently remove foreign particles out of the system. Blood veins limit particle size below 250 nm [67] since bigger particles would block smallest vessels. For therapeutic purposes particle size should decrease below 200 to gain effective tumor accumulation [56]. On other hand too small particles ($<$ nm) can pass the renal filtration and they are excreted [68, 69].

Particles bigger than 100 nm are rapidly (within seconds to minutes [18]) cleared from circulation through RES (reticuloendothelial system) [68]. The clearance has been shown to depend on the size, i.e. when particle size increases the clearance gets stronger [17]. Reticuloendothelial system is part of immune system where foreign material is recognized by e.g. macrophages or liver Kupffer cells which removes them from circulation with phagocytosis and by transporting them e.g. to the liver or spleen for degradation and excretion. The identification of foreign particles happens by blood protein, opsonin, adsorption on the surface (process referred as opsonization) [15, 70].

Considering all mentioned effects would leave only particles between 5 to 100 nm suitable for intravenous drug delivery, therapy and imaging applications. And still even if particles would be below 100 they would be cleared quickly from circulation by RES. Small size in porous particles would also decrease possible drug amount carried of one particle and increase the amount of particles needed to carry suitable drug dose. In addition as particle size decreases the manufacture becomes more laborious and as more particles are needed the amount of silicic acid from dissolution of silicon would get higher and could cause toxic effects. Particle sizes that would give best compromise between these factors would be about 60-200 nm.

Porous silicon particles however aggregates easily because of their high surface-to-volume ratio which occurs strongly at comparatively small particles ($<$ 220 nm) [67]. In this thesis we are speaking always of aggregation when particles are sticking to each other and forming bigger particles. Correct term would be affected by the way the particles are connected to each other, e.g. agglomerate when particles are held together by physical force and aggregate when they are stuck together via chemical

bonding. Identification between connection types is difficult and here we refer all particles that have stuck to each other as aggregates and reaction as aggregation.

Aggregation naturally affects the particle behavior in blood as particles get bigger and get stuck on small blood veins, e.g. in lungs and liver. This can cause major complications, and is therefore unwanted. RES also removes bigger porous silicon particles rapidly from circulation. Removal of hydrophobic particles by RES is even faster than hydrophilic [15, 21, 71], so hydrophilic surface chemistry is more preferable and can be done with surface modifications spoken in chapter 2.3.

The surface charge also affects much on the recognition of the particles and the following phagocytosis. Studies show that it is more preferred to have negative surface charge on particles [57, 72, 73, 74], i.e. recognition is not as efficient as with positive particles. The best option, considering RES, would however be neutral particles as it has shown to prevent recognition and phagocytosis efficiently on *in vitro* tests [21, 57, 72, 75].

On other hand study done by Roser et al. [72] indicates that surface charge of albumin nanoparticles doesn't make difference in circulation times as every particle had same clearance. In another studies done by Souris et al. [74], Lee et al. [76] and Wu et al. [77] indicate that surface charge of silica particles plays crucial role on clearance from blood stream. It was found that positive particles [74] had much faster clearance than those with negative surface charge [76, 77].

These different results indicate that *in vitro* situation differs from *in vivo* situation and needs profound investigation. In addition to surface charge, which can be modified with adding molecules on surface of original material, the composition of the core seems to be essential when determining blood circulation [57].

While neutral surface charges would be preferable for avoiding the RES it might lead to particle aggregation. According to DLVO-theory (Derjaquin-Landau-Verwey-Overbeek) [78, 79, 80] the neutral charge is harmful when speaking of particle stability. We're not going to discuss the DLVO-theory in detail here as it is enough for us to understand the basics of it. According to DLVO-theory, the particles interact with each other through electrical forces. Particles attract each other by van der Waals (vdW) forces and repels each other by Born force, which is due to overlapping electron orbitals. The van der Waals attraction is much stronger than Borne repulsion so the sum of these forces would induce aggregation.

However particles have also surface charges that are linked to the material and its properties. If particles from same material have strong surface charge (negative or positive) the particles repulse each other via electrostatic forces. When vdW force and electrostatic repulsion counteract each other (Borne usually neglected) the particles will no longer stuck on each other. Thereby high surface charge is desirable to achieve high electrostatic repulsion.

Even quite high surface charges can't however always prevent aggregation. This can be seen with e.g. oxidized porous silicon (TOPSI-OH) that have surface charge of -30 mV in PBS (phophate buffered saline), but they are still rapidly aggregated.

According the DLVO theory the dispersion concentration and particle size also affect the aggregation. This is due the fact that in high concentrated dispersion particles are closer to each other and collide other particles more frequently while they move (Brownian movement). At bigger size particles encounter more frequently with other particles which may cause aggregation.

Nonetheless when thinking RES the high surface charge would not be best choice for particles. Most of studies indicate neutral charge is best choice for particles but it might not be enough to prevent opsonization and on the other hand even high surface charge can't prevent aggregation. However surface of porous silicon can be modified to prevent these effects. One of the best and most used would be PEGylation of the particles which is discussed next.

3.1.1 The effect of PEGylation

Attaching PEG molecules to the surface of different nanoparticles have shown to be very efficient in reducing aggregation, protein adsorption, phagocytosis, clearance from blood circulation and therefore increasing circulation time of PEGylated particles [16, 17, 18, 20, 21, 22, 73, 81]. On other hand adding targeting ligands on PEG-molecules have shown to improve their uptake of desired cells [55].

Attaching PEG-molecules modifies the surface charge of particles [17]. PEG molecules are quite neutral [68] or slightly positive so they usually shift surface charge to more positive due to electric hindrance of PEG molecule layer [70, 71]. Neutral surface charges, that are beneficial considering RES, can be obtained with successful PEGylation. Neutrality might however result, according DLVO-theory, in aggregation of the particles.

Nonetheless it has been shown that PEGylation successfully reduces aggregation no matter what surface charge the particles have [16]. This study indicated that surface charge of PEGylated particles doesn't have any effect on aggregation. The repressed aggregation was due the steric hindrance that PEG coating makes to the particle surface.

In addition to neutral charge, the PEG-layer has been shown to prevent opsonization (Fig. 10). PEG-molecules are hydrophilic which is one of main factors, in addition to neutrality, in reducing protein adsorption to the surface [21, 70, 71]. Studies show that already short PEG ($<$ 1 kDa molecular weight) molecules are capable to prevent protein adsorption [21, 50, 82]. However many studies indicate that PEG chain length as well as layer density are two factors that are critical in preventing protein adsorption [17, 18, 20, 21, 22, 81, 82].

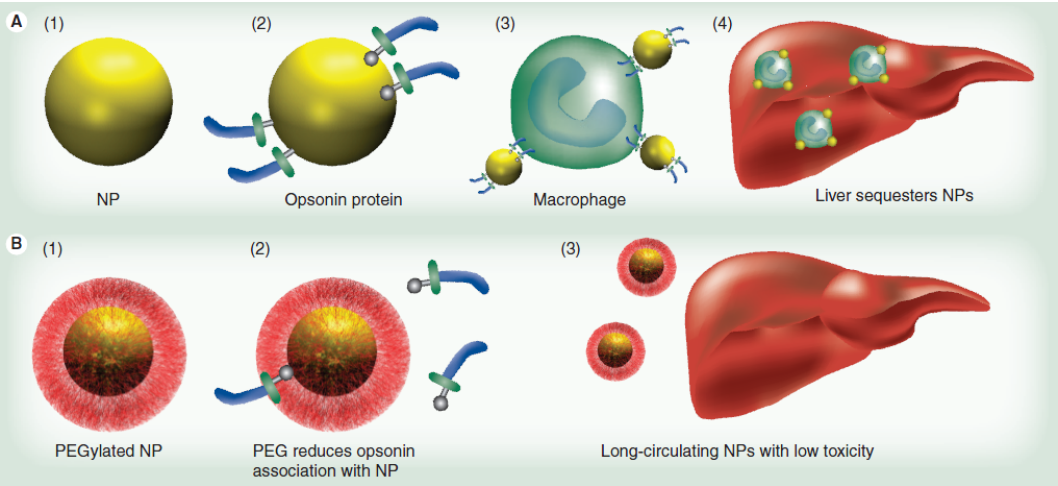

Figure 10: Schematic picture presenting how PEGylation affects particle behavior in blood stream. In A) (upper pictorial) it can be seen that opsonins are adsorbing to the surface of nanoparticles which are then detected and removed to the RES organs such as liver. In B) (lower pictorial) the PEGylation prevents the adsorption of opsonins and the particles can circulate in blood stream for longer times. [15]

The PEG length and surface density affect greatly the conformation that PEG molecules take on particle surface. Low molecular weight PEGs ($<$ 1 kDa) are supposed to form brush-like layer and bigger PEGs tend to from mushroom-like layer (Fig. 11) [19]. Also surface density of PEG affect much on forming composition as dense coatings exhibit brush-like layers and sparse coatings mushroom-like layers [19, 81].

Studies have shown that the protein adsorption decreases strongly in high density coatings [20]. On other hand you can't increase PEG density forever. It has been

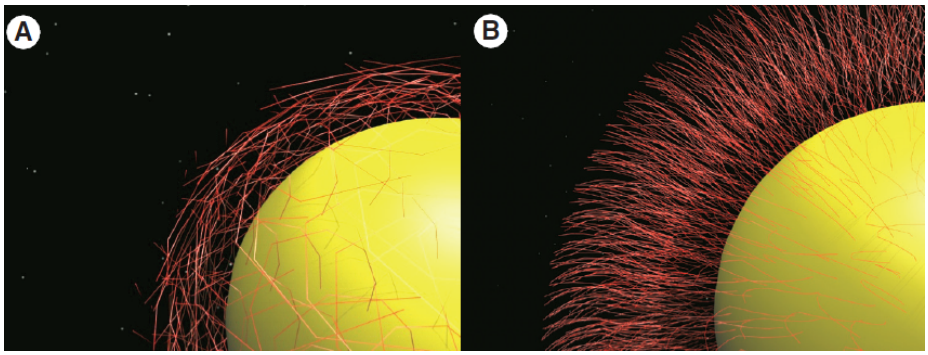

Figure 11: Illustrative picture representing A) mushroom-like formation B) brush-like formation of PEG on particle. [15]

showed that after certain threshold level the protein adsorption does not decrease and might even increases a bit [22, 81]. As the surface gets closer to be totally coated with PEG molecules, the PEG chains no longer have room to move and they lose their flexibility which have been supposed one of main reasons why PEG prevents effectively protein adsorption [81].

For PEG layer the flexibility and hydrophilicity increase with increasing chain length. These two parameters seem to be very important when considering good PEGylations. Storm et al. [83] report that PEG layer thickness should be at least 5 % of the original particle diameter to have steric effect, whereas others have studied the effect of grafting densities of different size of PEGs to find best density [20, 22, 81].

Jeon et al. [84] have submitted theory why PEGylation is good for preventing protein adsorption. According to this theory the PEG chains interact with the proteins. As proteins get closer to the PEG coated particles, the vdW force increases and proteins try to push through the PEG layer. As a result, the PEG layer is compressed into condensed high energy conformation. This change emerges repulsive force that can, if great enough, push protein away from the surface. The repulsive force is affected by PEG chain length and grafting density; bigger chain length and denser grid leads to bigger repulsive force. Same effect is most likely the reason for improved colloidal stability of PEGylated particles.

At low grafting density the core material is not fully coated with PEG and there might be enough room for proteins to adsorb on particle surface. On other hand too dense coating impairs flexibility and again proteins can adsorb to the surface. Critical thing for many applications and PEG lengths is to find suitable density between these extremities. However it seems that protein adsorption can't be totally

avoided no matter how particles are PEGylated. [22].

The effect of decreased protein adsorption can be seen from blood circulation tests and from studies which investigated the particle uptake of phagocytic cells. It has been shown by Fang et al. [17], Gref et al. [22] and He et al. [81] that particle phagocytosis is decreased as particles are PEGylated. The increased circulation has been shown by Fang et al. [17], Gref et al. [18] and Abuchowski et al. [85]. In studies done Fang et al. [17] the blood circulation time was increased from 28 min to 11.3 h of original and PEGylated particles, respectively.

In the same study the biodistribution of PEGylated particles was shown to shift more effectively towards tumors in mice. This is due reduction of accumulation to e.g. liver and spleen by RES. As the result the PEGylated particles can circulate longer in blood and accumulate to tumors due leaky vasculature of tumor tissue. Similar reduction on liver uptake (part of the RES) was seen on study done by Gref et al. [18], where 66 % of non-coated particles was accumulated in liver after 5 min of injection whereas after 5h less than 30 % of PEGylated particles had accumulated in liver.

From different studies it can be seen that longer PEG chains are more favorable on preventing clearance by RES and aggregation. However there are limitations on PEG chain length as they might increase particle size too much. PEG molecules are also non-biodegradable which can cause toxicity. PEG molecules have low toxicity [15, 57, 71] which is inversely proportional to molecular weight, which would suggest the use of longer PEG chains. However upper limit for PEG molecular weight is about 60 kDa but smaller PEGs ($<$ 20 kDa) are more beneficial for fast clearance [86]. Bigger, over 60 kDa, PEGs will accumulate in liver and can cause toxic effects. It has been estimated that acceptable daily intake of PEG is 0-10 mg/kg body weigth [71]. However the PEG length might affect much on the maximal daily intake.

PEG has also some other disadvantages such as immunogenicity [15, 71]. PEG is usually considered non-immunogenic as is prevents RES effectively but it still can lead to immune responses and to hypersensitivity reactions (HSR) [71]. However it is still unclear if PEG alone causes hypersensitivity or with combination of several factors [71]. Despite of PEGs disadvantages such as degrability under stress, toxic side-products and accelerated blood clearance (ABC) on repeated injections, its advantages are still much bigger as PEGylation has shown to decrease immunogenicity, antigenicity and toxicity [71].

4 Analyzing methods

The fabricated PSi and its properties such as particle size, surface charge and pore size need to be characterized for the optimal use of the material. Same applies for surface modifications, e.g. the amount of different molecules attached to PSi and their effect on properties such as pore size needs to be known. There are several different quantitative and qualitative methods that can be used for characterization. In this section few characterization methods are explained without going too deep in details.

4.1 Dynamic light scattering

Dynamic light scattering (DLS) is a easy and fast method for analyzing the particle sizes in dispersion. With DLS the possible particle aggregation can be seen as the detected particles get bigger over time. DLS exploits the Brownian motion of particles, i.e. the random movement of particles in dispersion. The basic measurement is done by targeting laser beam into the vial containing particles in desired medium. The laser source is usually low power laser such as He-Ne laser [87].

As laser beam hits particle it will be scattered in every direction. The scattered light will either hit another particles and scatter again or travel away from the medium and vial. The scattered light is then detected with photodetector which records the intensity of the incoming light. The old standard place for detecting the light would be at 90° but nowadays the detection is done at 173° angle (backscattering). The backscattering measurements are preferred as it gives better sensitivity and also higher particle concentrations can be used. In 90° angle measurements the light has to travel through medium which can obstruct its way if the medium is too concentrated. This is not a problem with backscattering measurements as particle sizes are measured close to the vial wall so light doesn't have to travel long distances in medium.

From detected intensity the particle size can be calculated with different theories. As mentioned the particles are randomly moving in the dispersion (Brownian movement) which causes them to collide into other particles. The speed of individual particle is affected by its size, i.e. bigger particles move slower than smaller ones.

In the measurement light is scattered to every direction as particles are pointed with laser beam. The light intensity scattered to the direction of the detector changes as particles are moving. The detected intensity is related to particle location respect to

the direction of incoming and reflected light. This intensity fluctuation is therefore directly related to the speed of the particles which is related to their size. This way the detected intensity can be used in calculations and the particle size distribution in the dispersion can be calculated. This size is called hydrodynamic size as the calculations assume particles to be spherical, which usually is not the case [88].

DLS is fast and reliable method for measuring particle size from dispersion. From individual measurement the size distribution and mean size can be obtained which are important parameters for intravenous dosing.

4.2 Gas sorption

Gas sorption is a measurement that is widely used in characterizing porous materials. It is quite accurate and with same measurement one can get information about pore size distribution, pore volume and surface area of the sample. Gas sorption is a measurement where sample of know material is exposed to gas at low temperatures. The sample is cooled and gas is dosed with controlled increments. The used gas is usually nitrogen, but also other gases such as krypton and argon can be used [27].

After stepwise increase in partial pressure of the applied gas, the pressure is allowed to equilibrate and the adsorbed gas amount is calculated. With the knowledge of adsorbed gas amounts in different pressures the adsorption isotherm can be drawn. As similar measurement is done backwards, i.e. dropping pressure to calculate how much gas is desorbed, the desorption isotherm can be drawn. By using sorption (adsorption and desorption) isotherm in calculations the material parameters such as pore diameter (average) and surface area can be calculated.

The pore size is one of the most important properties in many biomedical applications as it determines the behavior of loaded material. The pore diameter calculations usually done by using BJH (Barret-Joyner-Halenda)-theory [89]. Same theory is applied to pore volume and pore distribution calculations. Surface area is determined by using BET (Brunauer-Emmet-Teller)-theory [90].

The gas sorption method is used to characterize porous materials and e.g. the amount of loaded drug into the pores as it should decrease pore diameter and/or pore volume. This method is quite accurate but its disadvantage is that it can be accurately used only for microparticles and film samples. This is due the fact that small particles form pores between them which cause error to the results.

4.3 Fourier transform infrared spectroscopy

Fourier transform infrared spectroscopy, FTIR, is a measurement where the composition of measured sample can be obtained. The FTIR system uses an infrared light to measure the composition of the sample. This is done by targeting the light beam containing certain wavelength band into the material. The material absorbs some wavelengths according to what kind of bonds there are between the elements in the sample.

The light coming from the sample is detected with photodetector. The detected signal is raw data from the measurement which doesn't directly tell us what wavelengths have been absorbed nor their positions. To get this information the signal must be processed and this is done with Fourier transformation. As a result we get spectrum of light showing peaks in positions where absorbance has happened.

From this spectrum and the positions of absorbance, the composition of material can be analyzed. The different light absorbtion of molecules is caused by difference in the molecular vibrations which makes various bonds between elements to absord different wavelengths. Table 2 [26] shows some typical peak absorbance positions of porous silicon and the species that are associated with them.

Table 2: Absorbance peak positions of porous silicon and species associated with these peaks. [26]

Peak position cm^{-1}	Associated species	Peak position cm^{-1}	Associated species
465-480	SiO-Si bending	1463	CH_3 asymmetric deformed
611-619	Si-Si (bonds)	1720	CO
624-627	Si-H bending	2073-2090	SiH stretching (Si_3-SiH_3)
661-665	SiH wagging	2109-2120	SiH stretching (Si_2-SiH_2)
827	SiO bending (O-Si-O)	2139-2141	SiH stretching (Si-SiH_3)
856	SiH_2 wagging	2136-2160	SiH stretching (Si_2O-SiH)
878-880	Si-O or Si-O-H bending	2193-2197	SiH stretching (SiO_2-SiH)
905-915	SiH_2 bending	2238-2258	SiH stretching (O_3-SiH)
948	SiH bending (Si_2-H-SiH)	2856	CH sym. stretching (CH)
979	SiH bending (Si_2-H-SiH)	2860	CH sym. stretching (CH_2)
1061-1110	Si-O-Si asymmetric stretching	2921-2927	CH assym. stretching (CH_2)
1157-1170	surface oxide species	2958-2960	CH assym. stretching (CH_3)
1230	$SiCH_3$ bending	3450-3452	OH stretching (H_2O)
		3610	OH stretching (SiOH)

As can be seen from the Table 2, some wavelength areas overlap each other which complicates the analysis. However FTIR gives results that are sufficient for analyzing different materials on the sample. This method is usually used to verify the existence of some substance added to porous silicon. This way one can assume which peaks should be found and possible verify this with FTIR.

4.4 Thermogravimetric analysis

Thermogravimetric analysis, TGA, is a measurement which is used to quantify the amount (wt%) of added molecules to porous silicon. This means e.g. determination of the amount of PEG-molecules added to the PSi surface. Thermogravimetry, TG, is a device that is used to heat up the sample to high temperatures. The device weights the sample mass during the measurement to see whether there is any change. So basically TG has two components: an oven and a scale.

The measurement is based on weight loss of the sample when it is heated up. Different molecules have different temperatures where they decompose. When temperature is increased enough, the molecules attached to porous silicon surface will decompose and desorb out from the surface which will lead to mass decrease of the sample.

From the measurements a decomposition curve is drawn where the weight loss as a function of temperature is shown. From this curve the weight loss (wt%) can be calculated. Usually the material loses water and oxidizes in the process so for the real wt% of decomposed substance a reference sample without any added substance needs to be measured. As a result the real mass difference can be calculated.

4.5 Surface charge measurement

Surface charge is one of the most important factor when considering colloidal stability and the material behavior in blood circulation. All particles have usually electrical charge which is due their properties and structure. Surface charge is defined as electric charge at the particle surface and it can be caused e.g. by surface protonation/deprotonation and ion attachment.

Therefore the medium where particles are suspended affect the surface charge of particle. Different mediums have variety of ions which might attach to the particle surface due the electrical forces between these ions and particles and the pH of medium

affects the protonation/deprotonation process. This is the main reason why particles seem to have different surface charge in different mediums.

As the particles are suspended in medium, the ions of the medium can attach to the surface if it is electrically favored, i.e. positive ions are attached to negative particles and create positive layer on the surface. Because of the electrical charge, the ions bounded this way are strongly attached to the surface and this ion layer is called Stern layer. As we move further away from the particle a second, so called diffuse layer of ions is formed. This layer is more loosely bounded and it is same charged as the first layer, i.e. in case of negative particle the first two layers are positively charged. [91]

The combination of these layers is called electrical double layer which ends at the slipping plane. When the particle moves, the ions inside the slipping plane move with the particle but the ions outside the plane do not. The surface charge is measured from the slipping plane and it is called Z-potential [91]. The particle-ion system and the place for Z-potential measurement is show at Fig. 12.

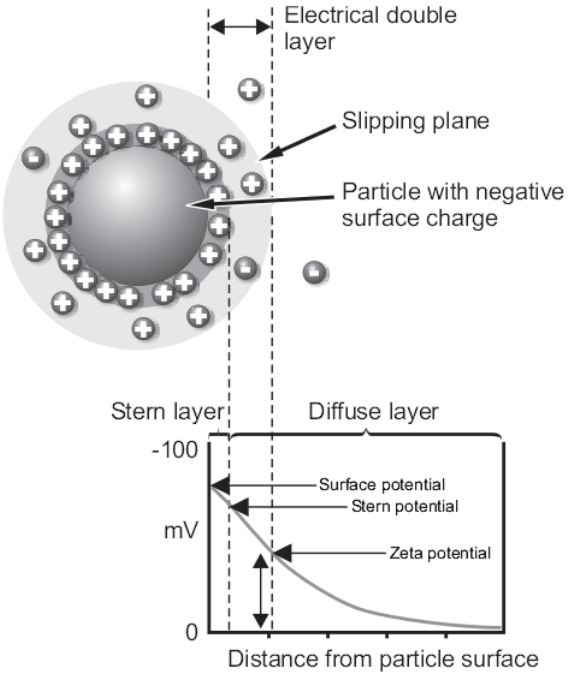

Figure 12: Illustrative picture showing how positive ions attach to negative particle. [91]

The Z-potential is measured then by combination of electrophoresis and laser Doppler velocimetry (LDV) and the whole method can be referred as laser Doppler electrophoresis (LDE) [91]. By using these two methods the velocity of the particles in the

medium is measured when electrical field is applied. The velocity of the particles is obviously related to the charge of the particles and the applied electric field. With the knowledge of medium viscosity, dielectric constant and the measured velocity of particles under known electric field the Z-potential can be calculated. So the measurement doesn't directly measure surface charge but the Z-potential which is proportional to it.

The measurement is widely used as it is fast and easy to perform. This method is used to measure the surface charge of the material which affects its behavior. With Z-potential measurements also the effect of substances loaded into or to the surface of the porous silicon can be evaluated, e.g. in case of PEGylation the decrease of Z-potential can be seen.

5 Experimental section

In this section, the experimental work done to study porous silicon behavior *in vitro* situation is explained. The study can be roughly divided into two parts; preliminary studies and long term stability studies.

In preliminary studies the work is done with porous silicon films, which were PEGylated with three different sizes of PEG to test whether PEG was attached to the surface of the PSi films or not. Two differently modified films, TOPSi-OH (thermally and chemically oxidized PSi) and TCHPSi-OH (thermally hydrocarbonized and chemically oxidized PSi), were used to test the possible PEG attachment.

In the long term stability tests the PSi nanoparticles with two different modifications (TOPSi-OH and THCPSi-OH) were used for colloidal stability testing. In the studies three different sizes of PEG were attached to the surface and the size of PEGylated nanoparticles was monitored for several days. To simulate blood, the particles were dispersed in PBS and incubated at 37 °C. Finally for imaging possibilities, suitable molecules were attached to PEGylated PSi particles. These molecules could be labelled with radioactive iodine which could be detected on *in vivo* tests.

5.1 Materials and methods

5.1.1 Preparation of porous silicon

Two different kind of materials were used in the exprerimental section; PSi films and PSi nanoparticles. PSi films were used in preliminary testing to detect the attached molecules and PSi nanoparticles were used for long term colloidal stability studies. For preliminary testing, large silicon wafers ([100] oriented, boron doped, diameter 15 cm, resistivity 0.01-0.02 Ωcm) were obtained from Okmetic. The porous silicon films were obtained by anodizing the Si-wafers for 40 min with current density of 40 mA/cm^2. The used electrolyte was 1:1 (v/v) hydrofluoric acid (38%)-ethanol. The obtained porous layer was detached from Si-wafer with high electric pulses (current densities of 150 mA/cm^2 and 250 mA/cm^2 were, respectively, used for 4 s and 3 s). After anodization the PSi films were collected from the surface of Si-wafer and dried at 65 °C.

For long term stability testing, small silicon wafers ([100] oriented, boron doped, diameter 10 cm, resistivity 0.01-0.02 Ωcm) were obtained from Siegert Wafer GmbH.

Wafers were etched with pulsed sequence for 20 min at 1:1 (v/v) hydrofluoric acid (38%)-ethanol solution. The pulse sequence was 50 mA/cm^2 for 2200 ms, 200 mA/cm^2 for 350 ms and waiting time of 1000 ms before repeating the sequence again. Obtained porous film was detached with high electric pulses and dried similar to the method in previous paragraph. Dried films were then milled with ball mill (Planetary Micro Mill, Pulverisette 7 premium line, Fritch GmbH) to obtain nanoparticles.

5.1.2 Surface modifications

The surface of PSi (films or particles) was then modified with either by thermal oxidation or thermal hydrocarbonization to have TOPSi and THCPSi, respectively. Thermal oxidation was done at 300 °C for 2 h in ambient air. Thermal hydrocarbonization is a process that has multiple steps:

1. Nitrogen (N_2) gas flushing at room temperature for for 30 min.
2. N_2 and acetylene (C_2H_2) gas flow at room temperature for 15 min.
3. Heating in oven with N_2 and C_2H_2 gas flow at 500 °C for 14 min 30 s.
4. Heating in oven with N_2 gas flow at at 500 °C for 30 s.
5. Cooling to room temperature under N_2 gas flow.

TOPSi and THCPSi were then chemically oxidized by either of two different methods:

Method 1

1. Oxidation with H_2O_2:HCl:H_2O (1:1:6 volume ratio) solution for 15 min at 85 °C.

- Washing the samples by using sonication twice with ethanol and twice with H_2O.

Method 2

1. Oxidation with NH_4OH:H_2O_2:H_2O (1:1:6 volume ratio) solution for 5 min at 85 °C.

    - Washing the samples by using sonication twice with H_2O.

2. Oxidation with H_2O_2:HCl:H_2O (1:1:6 volume ratio) solution 15 min at 85°C.

- Washing the samples by using sonication twice with ethanol and twice H_2O.

The materials manufactured this way are referred as TOPSi-OH and THCPSi-OH.

5.1.3 PEGylation

The PEGylation was done by utilizing silanol chemistries. With this method the PEG molecules are attached to the existing hydroxyl groups. 0.5 kDa mPEG-silane (Methoxy(polyethyleneoxy)propyltrimethoxysilane, 90 %, 9-12 PE-units) was obtained from ABCR GmbH & Co. KG, 2 kDa mPEG-silane and 10 kDa mPEG-silane were obtained from Laysan Bio, Inc.

The PEGylation was done with reflux method at 120 °C. The PSi samples were dried at 85 °C in vacuum prior to PEGylation to evaporate water off. Toluene was used as solvent because its water extracting ability [92] and thus yielding better PEG coating. The reaction solvent and the PSi were flushed with N_2 gas flow for 30 min before turning the heat on. The PEGylation was continued overnight (> 18 h). After PEGylation the sample was washed twice with ethanol and twice with H_2O. Figure 13 illustrates the whole process made for PSi to produce PEGylated TOPSi.

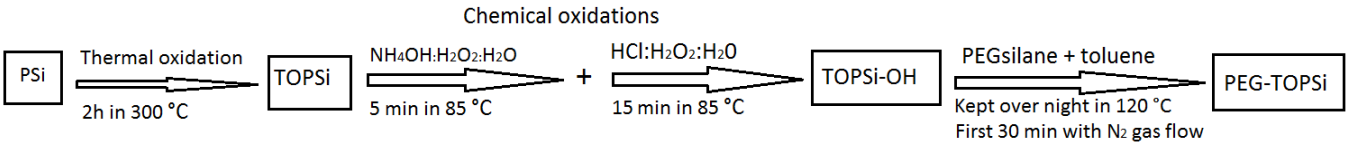

Figure 13: Schematic picture of PSi preparation to PEG-TOPSi

At the start of the experimental work the PEGylated sample was washed twice with ethanol and twice with H_2O. At the final experiments the reaction solvent was evaporated as it was seen to improve the results. Similar washings were done to these samples as well (two times with ethanol and two times with H_2O).

In addition to PEGylating the sample with one sized PEG molecules, also PEGylation at the same time with two different size of PEG molecules (0.5 kDa and 2 kDa) were done. The best PEG:TOPSi/THCPSi ratio was found to be 1 ml of 0.5 kDa mPEG-silane to 150 mg TOPSi/THCPSi and 5:1 ratio for 2 kDa and 10 kDa mPEG-silane to TOPSi/THCPSi particles.

5.1.4 Addition of suitable molecules for imaging

For imaging possibilities, the effect of two different molecule attachment to the colloidal stability was evaluated. PEGylated TOPSi particles were modified with either APTES ($\geq$ 98 %, M=221.37 g/mol, Sigma-Aldrich) or Triethoxy(4-methoxyphenyl) silane (97 %, M=270.4 g/mol, Sigma-Aldrich). For later purposes the latter compound is referred as Phenyl.

The attachment of these molecules were done with refluxation at 120 °C for 3h. Toluene-ethanol (5:1 v/v) mixture was used as solvent. The reaction solvent and the PEGylated PSi were flushed with N_2 gas flow for 30 min before turning the heat on. The amount of APTES or Phenyl was kept low as it is not necessary to have excess of these compounds at the surface for imaging purposes. The samples washed after the process twice with ethanol and twice with H_2O.

5.1.5 Analysis and characterization

The analysing methods included thermogravimetric analysis (Q50 TGA, TA Instruments), gas sorption (TriStar II 3020, Micromeritics), Fourier transform infrared spectroscopy (Nicolet 8700 FT-IR, Thermo Scientific), size and Z-potential measurements (Zetasizer Nano ZS, Malvern).

FTIR and gas sorption measurements were done only to film samples whereas TGA was done mostly on film samples but also on nanoparticles. In TGA the samples were heated up to 700°C in the presence of N_2 gas flow. At this temperature attached molecules are decomposed and desorped from the surface which leads to mass decrease of the sample. Nitrogen gas was used for measuring pore sizes and volumes in gas sorption. Prior to gas sorption the samples were dried in vacuum to remove impurities such as water. FTIR data was obtained with wavelengths varying from 400 cm^{-1} to 4000 cm^{-1}. The FTIR measurement were done in ambient air.

Size and Z-potential measurements were done only for nanoparticles. For long term stability measurements, the particles were dispersed either in water or PBS and Z-potential measurements were done in these mediums also. In long term stability studies the samples were incubated between the measurements at 37°C. The samples were sonicated before the first size measurement to ensure that particles weren't aggregated at the beginning. To see possible particle aggregation, the samples were only gently shaken before later measurements.

5.2 Results and discussion

5.2.1 Preliminary studies

First studies were done with film samples which were first thermally oxidized and then chemically oxidized with method 1. The manufactured TOPSi-OH films were PEGylated with 0.5 kDa mPEG-silane. The manufactured films were analyzed with TG and FTIR to verify the attached PEG molecules. Gas sorption was used to study whether PEGylation had effect on pore sizes and pore area. In measurements TOPSi-OH films were used as control.

The TGA results (Fig. 14) indicate the mass decrease of 1.07 wt% for TOPSi-OH films and 16.9 wt% for 0.5 kDa PEG-TOPSi films. The mass decrease observed in TOPSi-OH films is due the evaporating water and impurities. Also the sample oxidizes in the measurement which causes mass increase.

The mass decrease seen with 0.5 kDa PEG-TOPSi is partly due to same effects but mainly because of decomposition and desorption of PEG molecules. When taking into account changes of TOPSi-OH films and extracting this from PEG-TOPSi decrease, we obtain the value of 15.8 wt%. Therefore the amount of 0.5 kDa PEG polymer on PSi surface would be 15.8 wt%.

The nitrogen gas sorption measurements were done to TOPSi-OH films and 0.5 kDa PEG-TOPSi film to see whether the PEG coating is blocking or filling the pores and therefore resulting smaller pore size or decreased pore volume. The N_2 gas sorption results (Fig. 15) however indicate that the PEG-molecules do not completely fill the pores as the pore size is very similar in TOPSi and PEG-TOPSi films.

The average pore size and pore volume, calculated with BJH-theory from desorption isoterm, were 9.8 nm and 0.79 cm^3/g in TOPSi films whereas they were 11.3 nm and 0.84 cm^3/g in PEG-TOPSi. These results are very similar to each others and the small difference between these results might be due to the small inhomogeneity between properties of used films.

Finally the FTIR results indicate clear change between the composition of the measured TOPSi-OH films and 0.5 kDa PEG-TOPSi films (Fig. 16). We're not interested in the area below 1200 cm^{-1} since it is characteristic for porous silicon and it is pretty much the same on both samples.

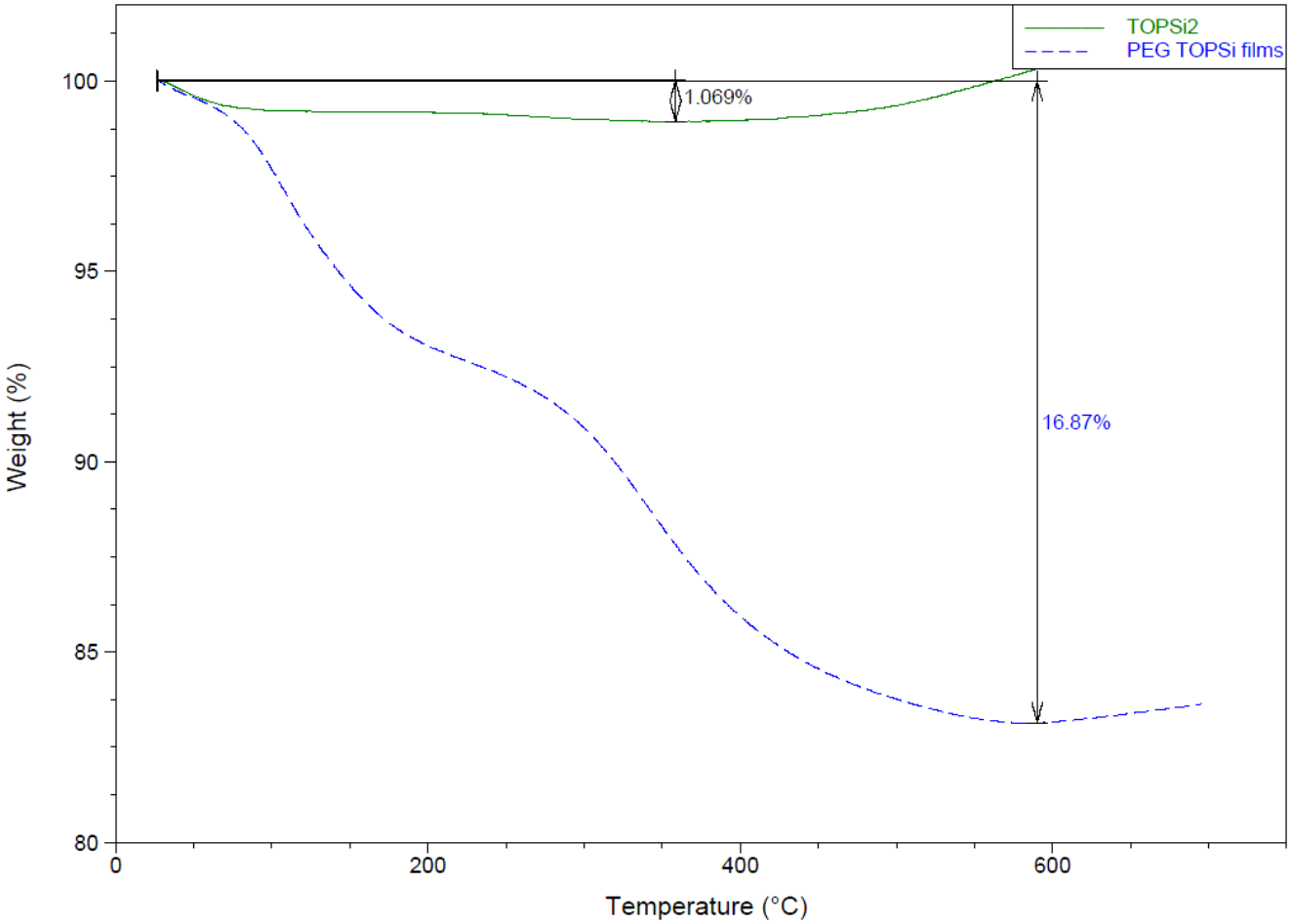

Figure 14: Thermogravimetric analysis results for 0.5 kDa PEG-TOPSi films and TOPSi-OH films.

First interesting peak is at 1300 cm^{-1} which is due C-O bonds of the PEG [93]. The next two detectable peaks 1350 cm^{-1} and 1455 cm^{-1} are due C-H bending and rocking in the PEG [26, 93].

2270 cm^{-1} peak is due Si-H bonds [94]. Its presence indicates poor oxidation of TOPSi but its reduction in PEGylated sample also prove the precence of added PEG. By poor oxidation we mean the effect of chemical oxidation which should have oxidized the Si-H groups as Si-OH groups. The strong 2870 cm^{-1} peak is due C-H bond streching in PEG and the broad peak at 3360 cm^{-1} is due water that is hydrogen bonded [26]. Although samples are dried in the oven, there are H_2O molecules presence as PEG is highly hydrophilic and there are a lot of water in the ambient air. The final peak at 3745 $^{-1}$ in the TOPSi-OH films indicates the existence of Si-OH groups and specifically vibration in O-H bonds [94]. Its elimination proves that PEG molecules are attaching to -OH groups on the surface.

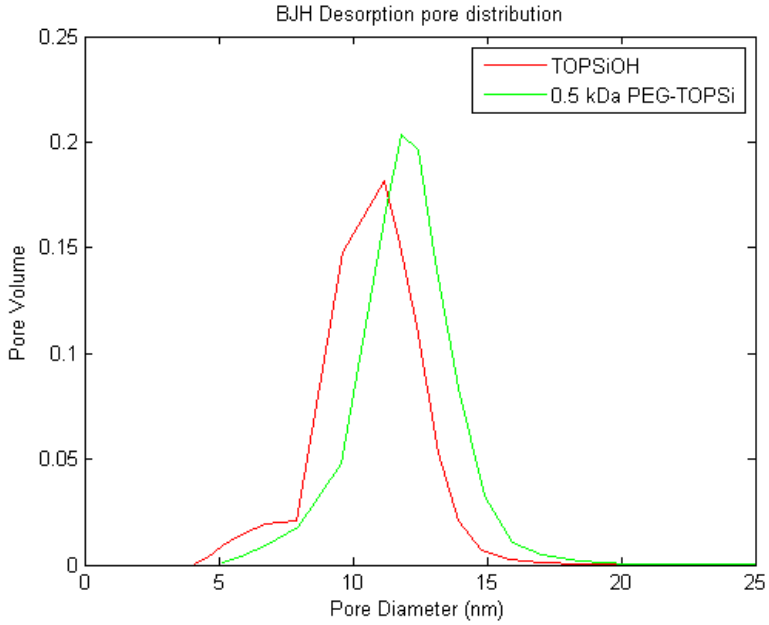

Figure 15: Results for N_2 gas sorption measurements of TOPSi-OH and 0.5 kDa PEG-TOPSi films.

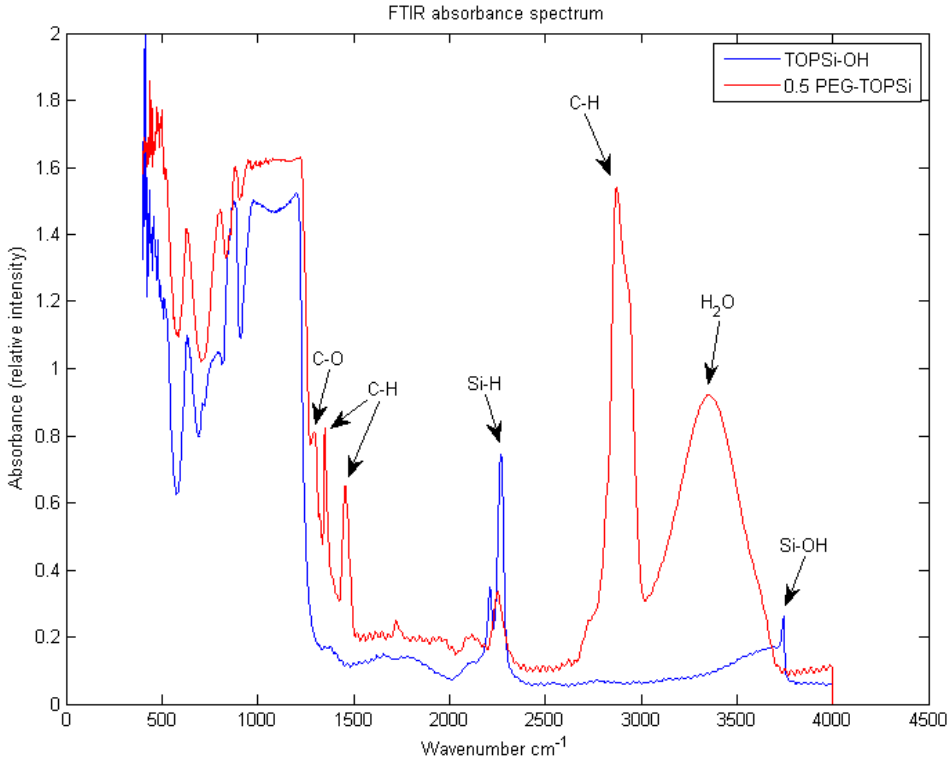

Figure 16: FTIR absorption spectrum for TOPSi-OH and 0.5 kDa PEG-TOPSi films.

Preliminary studies were continued by trying different sizes of PEG molecules in PEGylation and also by trying to PEGylate thermally hydrocarbonized PSi, THCPSi. However as previous FTIR results (Fig. 16) showed the presence of Si-H in the sample, the chemical oxidation was changed to method 2. By doing two chemical oxidations it was assumed that the amount of hydroxyl groups could be increased and better PEG coating could be obtained.

Now the PEGylation was done with 0.5 kDa, 2kDa and 10 kDa mPEG-silane to TOPSi-OH films. THCPSi-OH films were PEGylated with 0.5 kDa and 2 kDa mPEG-silane. Manufactured films were analyzed again with TGA, gas sorption and FTIR.

The TGA results for TOPSi films and THCPSi films are showed, respectively, in Fig. 17 and Fig. 18. As can be seen from Fig. 17 a decrease of mass was seen in every sample. For TOPSi-OH films the mass decrease was 1.28 wt%. This value is slighty bigger than previously which indicates the effect of the change done in chemical oxidations. For PEGylated samples the mass decreases were 14.8 wt%, 14.6 wt% and 18.7 wt% for 0.5 kDa, 2 kDa and 10 kDa PEG-TOPSi, respectively. The calculated PEG amounts are presented in Table 3

Table 3: PEG amounts (wt%) in 0.5 kDa PEG-TOPSi, 2 kDa PEG-TOPSi and 10 kDa PEG-TOPSi films

Sample	PEG wt%
0.5 kDa PEG-TOPSi	13.5
2 kDa PEG-TOPSi	13.3
10 kDa PEG-TOPSi	17.4

The results are logical in sense that the 10 kDa PEG-TOPSi had most PEG (wt%) on the particles. Reason why the amount of 0.5 kDa PEG was greater than 2 kDa can not be so easily explained. It can be due the fact that there are more PEG molecules in the reaction since the 0.5 mPEG-silane amount wasn't as well defined as for 2 kDa and 10 kDa mPEG-silane which had 1:5 ratio of PSi and mPEG-silane, respectively.

With 0.5 kDa PEG molecules, the surface of PSi might be fully covered whereas with 2 kDa and 10 kDa PEG the polymer chains might prevent dense attachment of PEG chains on the PSi surface. As a result only certain amount of PEG molecules can attach the surface and the PEG molecule weight causes the difference between the 2 kDa PEGylated and 10 kDa PEGylated films.

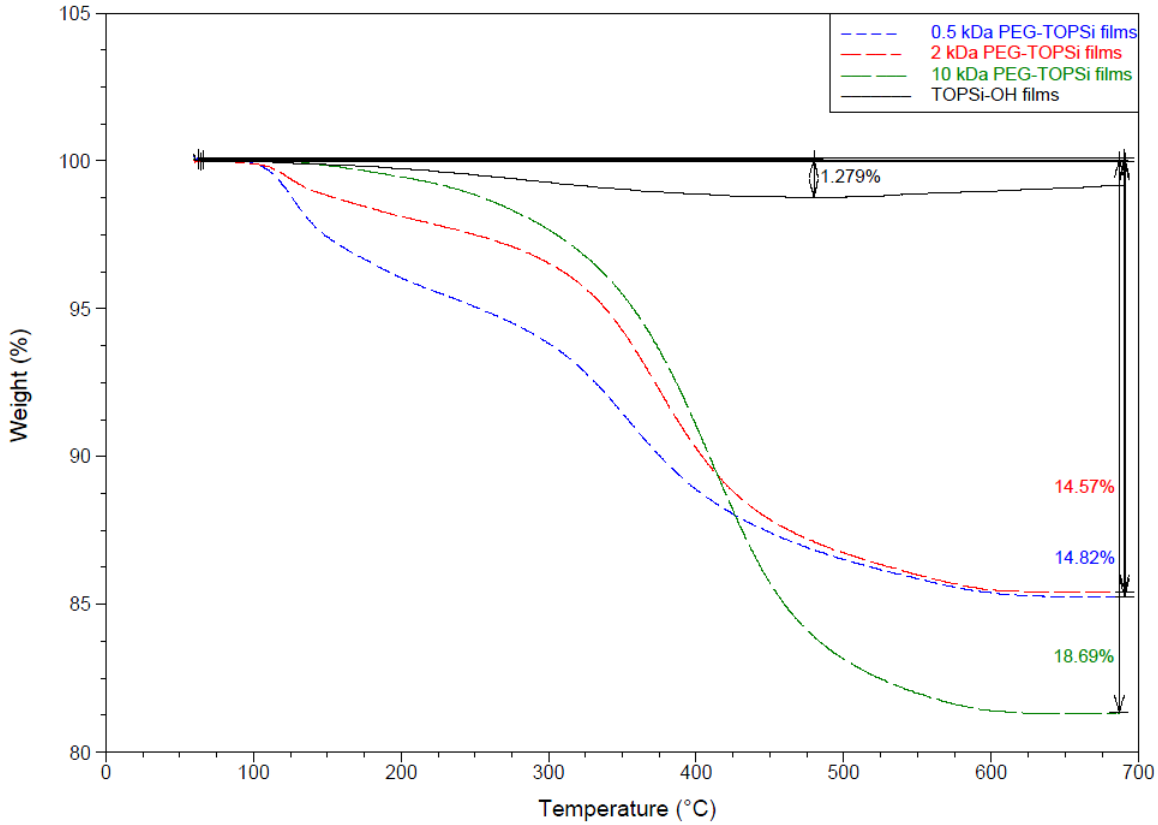

Figure 17: Thermogravimetric analysis results for 0.5 kDa, 2kDa & 10 kDa PEG-TOPSi films and TOPSi-OH films.

TGA results for THCPSi-OH films indicate that PEG molecules can be attached to the surface of THCPSi films (Fig. 18). The mass decreases were 1.64 wt%, 8.31 wt% and 15.6 wt% for THCPSi, 0.5 kDa PEG-THCPSi and 2 kDa PEG-THCPSi films, respectively. Calculated PEG amounts are presented in Table 4.

Table 4: PEG amounts (wt%) in 0.5 kDa PEG-THCPSi and 2 kDa PEG-THCPSi films

Sample	PEG wt%
0.5 kDa PEG-THCPSi	6.7
2 kDa PEG-THCPSi	13.9

The wt % amount of 2 kDa PEG molecules in THCPSi films seem to be very similar to TOPSi films. However the amount of 0.5 kDa PEG molecules in PEG-THCPSi films is much lower than in PEG-TOPSi films. This would indicate the limited amount of hydroxyl groups at the surface for PEG to attach. However if this was the only reason, the 0.5 kDa PEG amount (wt%) should be quarter of 2 kDa PEG amount

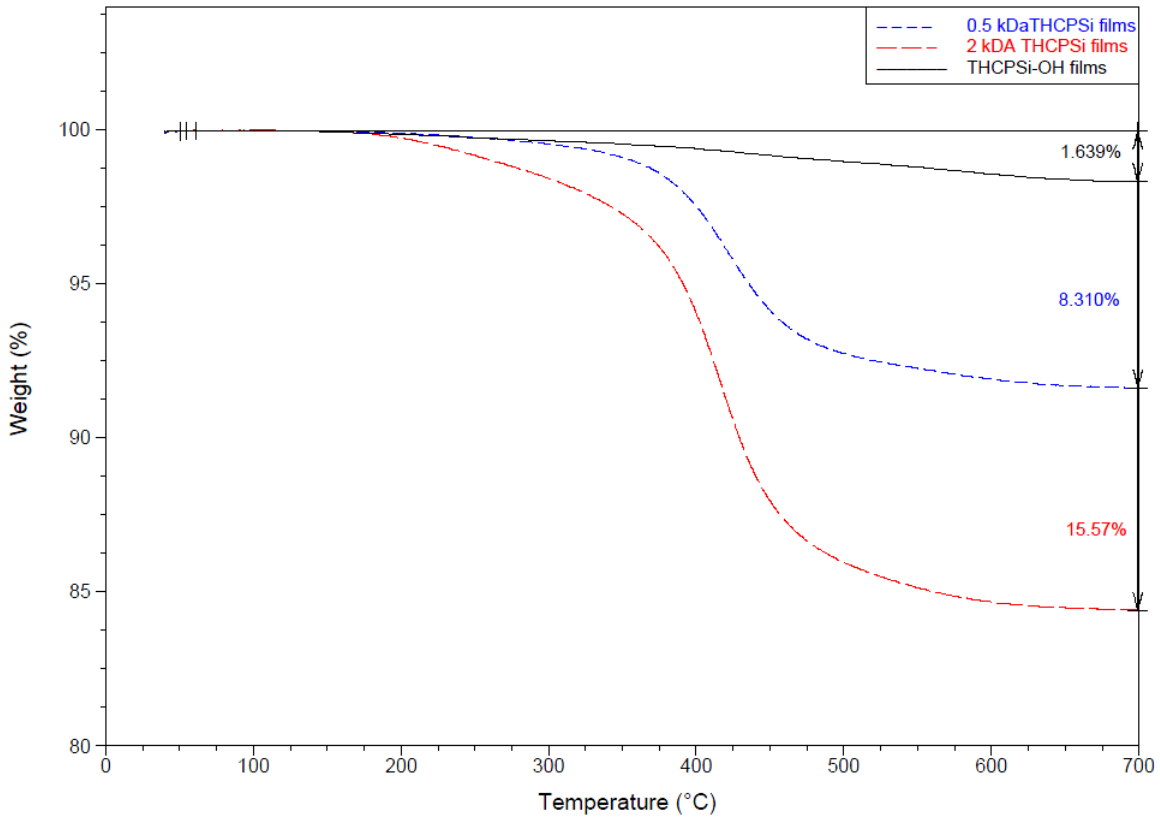

Figure 18: Thermogravimetric analysis results for 0.5 kDa & 2kDa PEG-THCPSi films and THCPSi-OH films.

(wt%). Again it could be due the fact that 2 kDa PEG polymer chains block the full coverage of the surface. Also as THCPSi particles are hydrophobic by nature the bonding with hydrophilic PEG might have been slightly prevented even though there are hydroxyl groups at the surface.

N_2 gas sorption results of TOPSi films show that pore diameter decreases a bit when particles are coated with PEG (Fig. 19 & Table 5). However it is hard to say whether PEG molecules are blocking the pores or is the deviation just because the inhomogeneity of the films or the partial filling of the pores. The pore sizes and pore volumes (calculated from desorption isoterm by using BJH-theory) of the TOPSi films are shown in Table 5.

The results listed in the Table 5 indicate that pore volumes have degreased significantly. As inhomogeneity explains some of the variations the mains reason however must be partial filling of the pores and the blockage of pores. From Table 5 it can be seen that pore volume decreases almost linearly with increase of PEG length, with the exception of 2 kDa PEG.

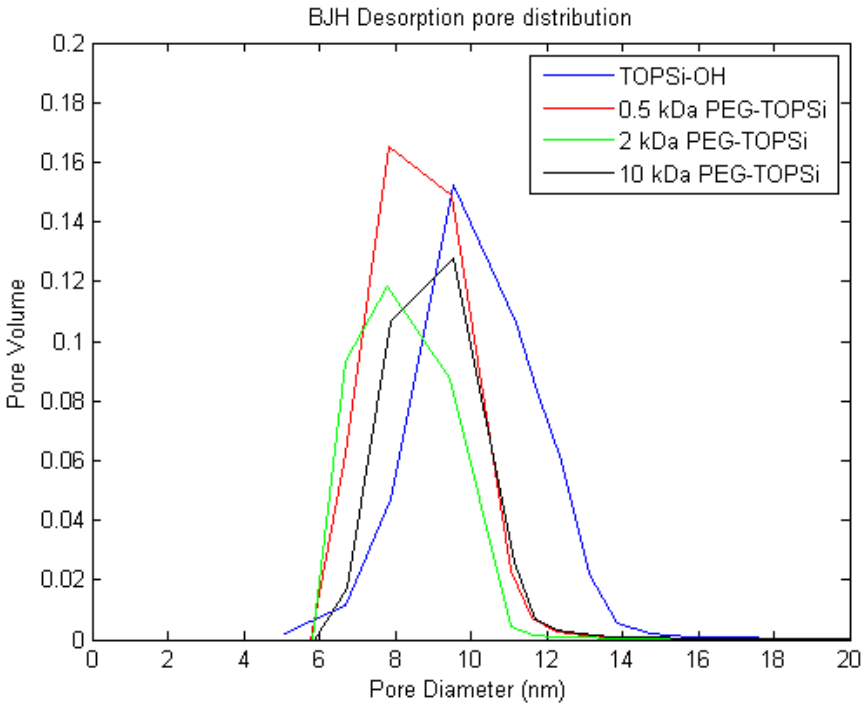

Figure 19: Results for N_2 gas sorption measurements of TOPSi-OH, 0.5 kDa PEG-TOPSi, 2 kDa PEG-TOPSi and 10 kDa PEG-TOPSi films.

Table 5: Pore size and pore volume obtained from N_2 gas sorption measurement done to TOPSi-OH, 0.5 kDa PEG-TOPSi, 2 kDa PEG-TOPSi and 10 kDa PEG-TOPSi films

Sample	Pore size (nm)	Pore volume (cm^3/g)
TOPSi-OH	9.4	0.7
0.5 kDa PEG-TOPSi	8.1	0.6
2 kDa PEG-TOPSi	7.6	0.4
10 kDa PEG-TOPSi	8.4	0.5

The different result for 2 kDa might be due the film homogeneity which also affects the detected pore sizes. Nonetheless the decrease of pore volumes would indicate that pores are partially blocked. The attachment point of PEG is also unclear. PEG chains might be attaching to the particle surface but also at pore walls which would decrease pore size and pore volumes. However PEG attachment would need more research work to find out the real reason for decreased pore size and volume. Also as there was no repeated measurement the results only give indicative values because the measurement errors can cause variations seen in Tables 5 and 6.

The results for PEGylated THCPSi films are shown in Fig. 20 and Table 6. Similarly pore diameter and pore volume has decreased after PEGylation with 2 kDa PEG molecules. Results for 0.5 kDa PEGylated THCPSi films are very close to THCPSi-OH films. This would indicate that either PEG molecules have been attached only to the surface and they would not block of fill any pores or that 0.5 kDa PEGylated films had bigger pores, due to inhomogeneity, before the PEGylation.

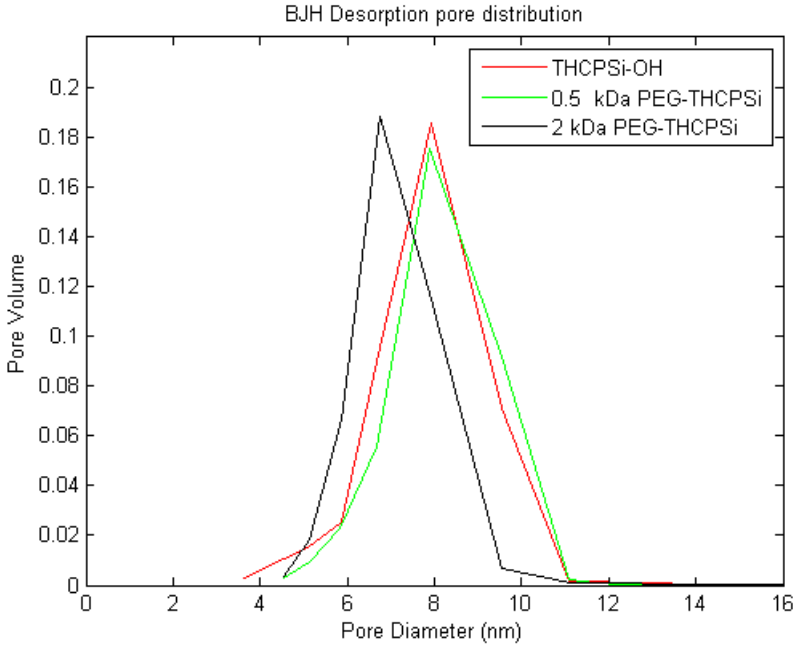

Figure 20: Results for N_2 gas sorption measurements of THCPSi-OH, 0.5 kDa PEG-THCPSi and 2 kDa PEG-THCPSi films.

Table 6: Pore size and pore volume obtained from N_2 gas sorption measurement done to TOPSi-OH, 0.5 kDa PEG-TOPSi, 2 kDa PEG-TOPSi and 10 kDa PEG-TOPSi films

Sample	Pore size (nm)	Pore volume (cm^3/g)
THCPSi-OH	7.2	0.5
0.5 kDa PEG-THCPSi	7.5	0.5
2 kDa PEG-THCPSi	6.6	0.4

Either way, comprehensive analysis cannot be done based on these measurement. What can be concluded is that pores and pore volumes are decreased in almost all the samples. The PEG molecules might be attaching to the pore surfaces and also blocking the pores. However these effects could be regulated by controlling the PEG amount at the process.

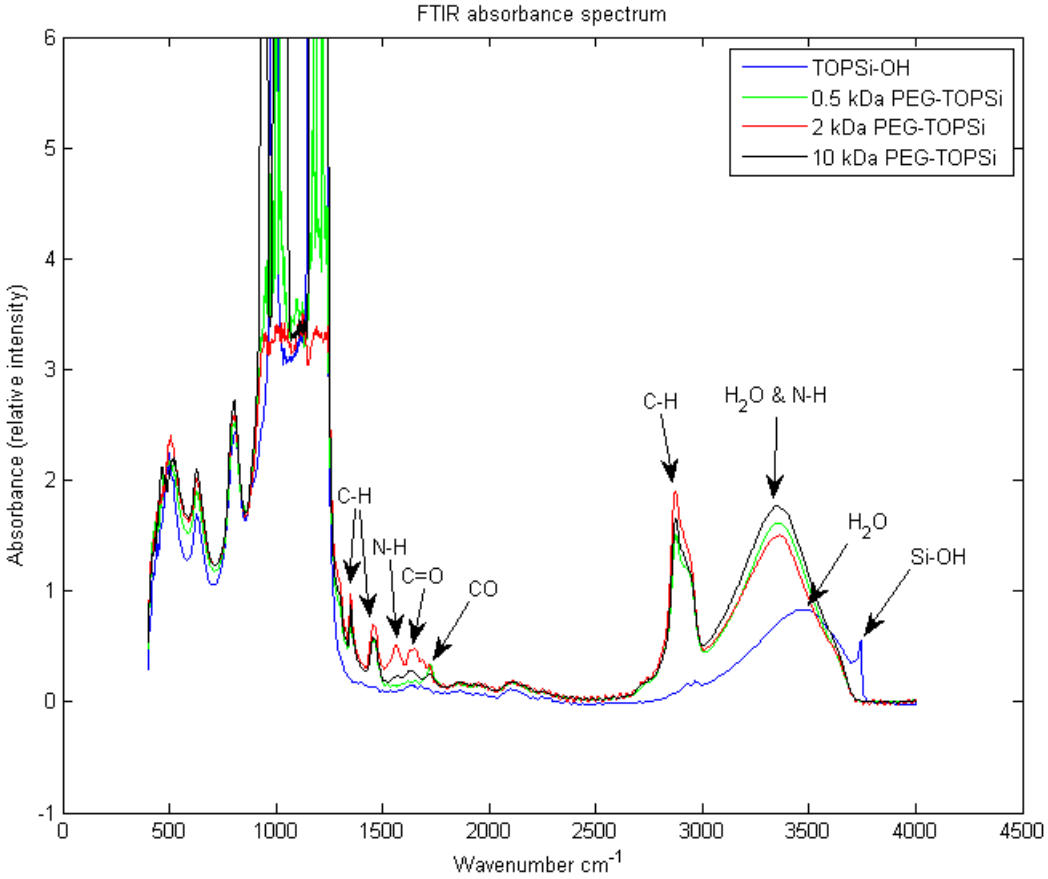

Figure 21: FTIR absorption spectrum for TOPSi-OH, 0.5 kDa PEG-TOPSi, 2 kDa PEG-TOPSi and 10 kDA PEG-TOPSi films.

The FTIR results for PEGylated TOPSi films and PEGylated THCPSi films are showed in Fig. 21 and Fig. 22, respectively. Again we are not interested in the area below 1200 cm^{-1} as it is charasteristic to used material.

Peaks 1350 m^{-1} and 1460 cm^{-1} indicate C-H bending in PEG. The 1560 cm^{-1} and 1659 cm^{-1} peaks, that only show in 2 kDa PEGylated and 10 kDa PEGylated sample, are due N-H bending and C=O stretching vibrations, respectively [93]. 1720 cm^{-1} peak is associated in CO species in PEG [26]. 2872 cm^{-1} is due C-H stretching, 3350 cm^{-1} is mostly due H_2O but it also buries N-H stretching peak under it in 2 kDa and 10 kDa PEGylated TOPSi films. The final peaks of TOPSi-OH film, 3500 cm^{-1} and 3740 cm^{-1}, are due H_2O and SiO-H vibrations, respectively.

Similar peaks were seen on PEGylated THCPSi samples (Fig. 22). 1250 cm^{-1} peak is associated with C-O bonds in PEG. Peak 1350 cm^{-1} and 1450 cm^{-1} are due C-H

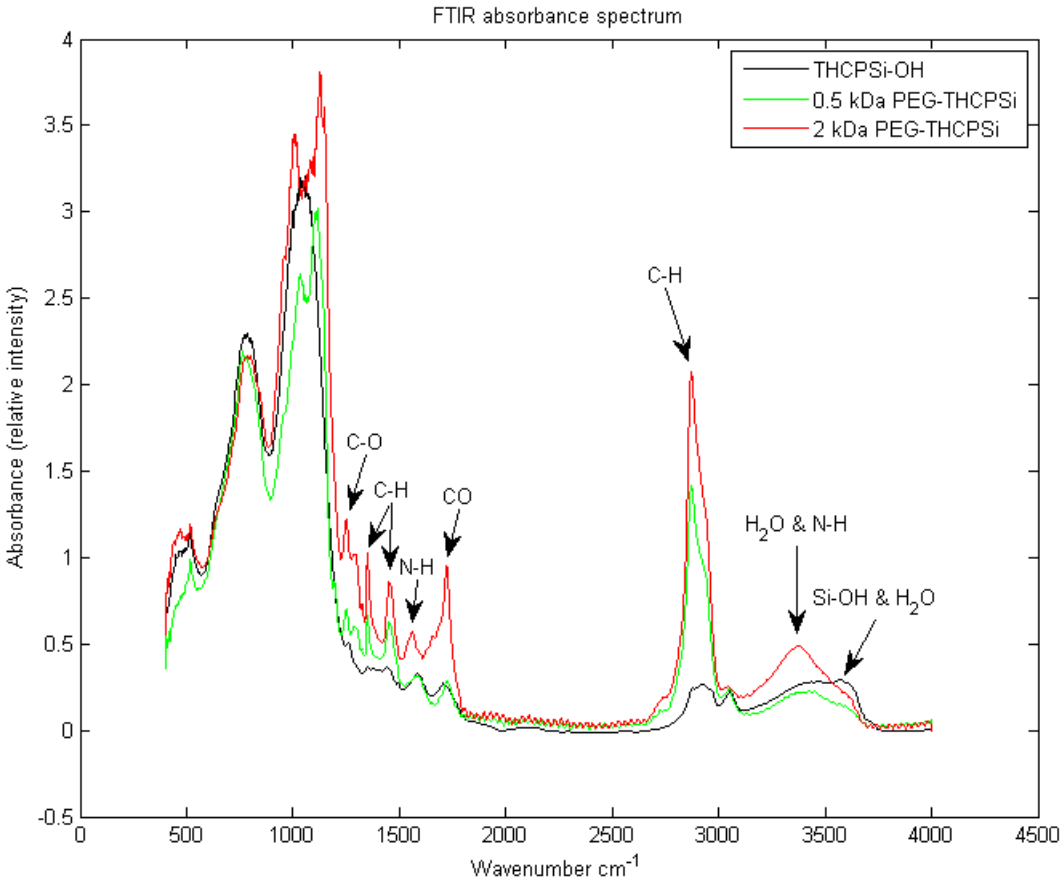

Figure 22: FTIR absorption spectrum for THCPSi-OH, 0.5 kDa PEG-THCPSi and 2 kDa PEG-THCPSi films.

bending. 1565 cm^{-1} and 1720 cm^{-1} peaks are due N-H bending and CO vibrations, respectively. The CO peak is stronger than with TOPSi as THCPSi has been modified to have C-H species at surface before it was chemically oxidized. 2873 cm^{-1} is due C-H stretching, 3370 cm^{-1} is mostly due H_2O but it also buries N-H stretching peak under it in 2 kDa PEGylated TOPSi films. The last peak of TOPSi-OH film, 3575 cm^{-1} is due SiO-H vibration which have been almost covered under the H_2O broad peak.

The result of preliminary studies clearly indicate that PEG molecules can be attached TOPSi-OH and THCPSi films. As results were positive the next step was to move into PEGylating nanoparticles and test their long term colloidal stability.

5.2.2 Long term stability studies

In long term stability studies main difference to preliminary tests was the use of nanoparticles. At the start the stability of non-PEGylated TOPSi-OH particles was tested in H_2O and in PBS which was used to simulate blood. It was seen that TOPSi-OH particles were stable in H_2O but aggregated rapidly in PBS (Fig. 23).

It could be seen that aggregation happened immediately as already at first measurement point the TOPSi-OH particles were 70 nm bigger than those in water. From these measurements it was clear that TOPSi-OH particles were not stable in PBS.

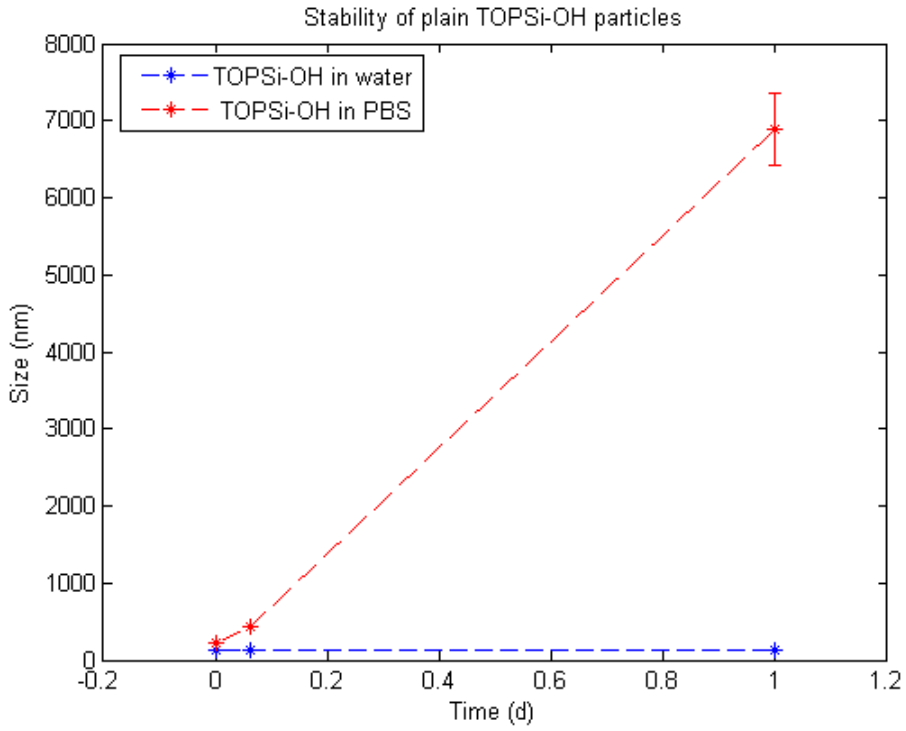

Figure 23: Initial situation regarding stability of TOPSi-OH in H_2O and PBS.

The ions in PBS adsorp to the surface of TOPSi-OH particles which alters the Z-potential. Z-potentials measured were -50 mV in water and -30 mV in PBS. Clearly the shift towards positive potential decreases the repulsive force of TOPSi-OH particles and the particles will aggregate.

The PEGylation was supposed to prevent aggregation and therefore its effect on colloidal stability was tested. The tests were firstly done to TOPSi particles as they are more suitable for drug delivery applications. First study done with 0.5 kDa PEG indicated that 0.5 kDa PEG molecules could not prevent aggregation (Fig. 24).

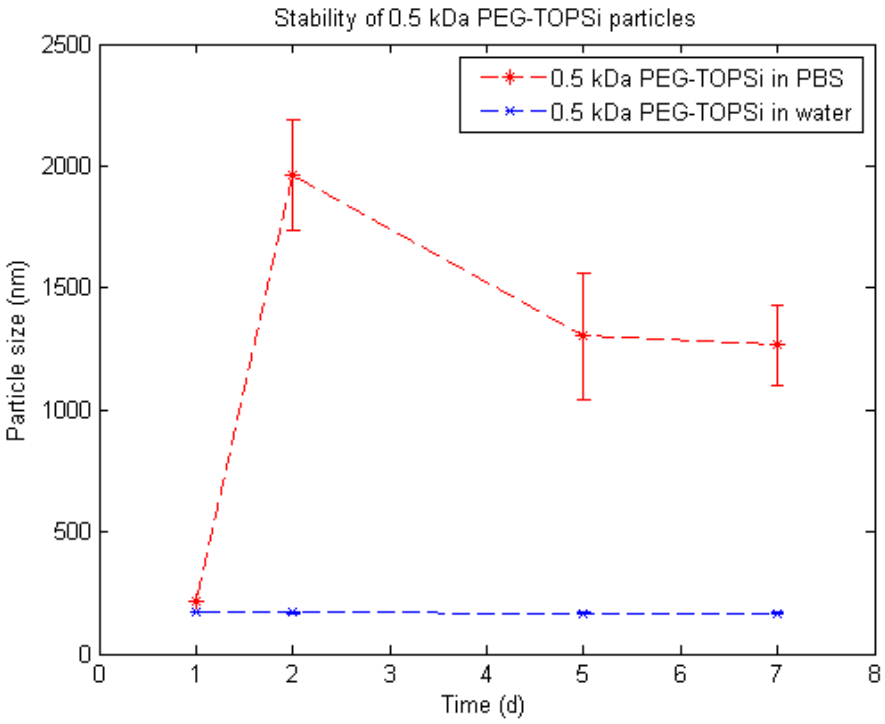

Figure 24: Stability of 0.5 kDa PEG-TOPSi in H_2O and PBS.

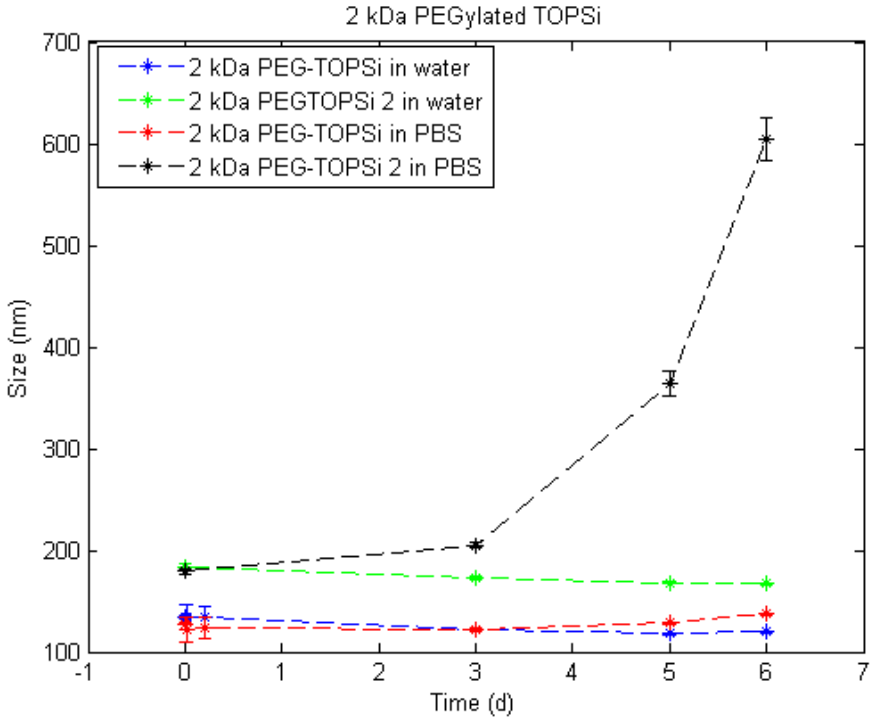

Figure 25: Stability of 2 kDa PEG-TOPSi in H_2O and PBS.

It was assumed that 0.5 kDa PEG chain length is not sufficient to form counter force strong enough to prevent aggregation. This counter force is formed as PEG chain is folded and naturally PEG tries to prevent this bending. However the PEGylation had some effect as aggregation was not that strong and the particle size seemed to stabilize to certain size. The next step was to PEGylate the samples with 2 kDa PEG which had longer polymer chain. The results of this PEGylation seemed to strengthen our hypothesis how chain length affects the stability as 2 kDa PEG was seen to prevent aggregation on smaller particles (Fig. 25).

It was observed that bigger particles aggregated after 3 days whereas smaller particles were stable for the whole measuring period. Nonetheless the results were much better than with 0.5 kDa PEGylation and it seemed that PEG chain length had crucial effect on stability of the particles. Now the PEG chains were able to form counter force strong enough for preventing the aggregation of small particles. In the PEGylation process the reaction solvent had been evaporized which may have some effect on the stability. This was however neglected as it was assumed that only PEG chain length is responsible for positive effects.

To do final test on this hypothesis, TOPSi-OH particles were PEGylated with 10 kDa PEG which was assumed to be able to prevent aggregation of bigger particles. The results of stability measurements (Fig. 26) for these particles were obviously worse which wrecked the hypothesis. The reason why PEGylation with 10 kDa PEG was unsuccessful is not fully understood.

One possible reason could be the chain length of 10 kDa PEG. These PEGs could have too long chain which would prevent effective surface coverage. The coating could be so sparse that particles would be able to interact with each other normally. Another explanation is just the opposite; PEG coating was too effective which led to decrease in chain mobility [83]. As the mobility decreases, the steric hinderance effect also decreases which might lead to aggregation.

The study done Gref et al. [22] would be against the latter hypothesis. In their study it was seen that while increasing the PEG length the necessary grafting density needed to reduce protein adsorption decreased. However in this study they did not found upper limit for grafting density. As they increased grafting densities up to 20 wt% the protein adsorption was at same level as with 5 wt%. The protein adsorption was shown to increase when using grafting densities of PEG below 5 wt%, which was the threshold limit for 5 kDa PEG to have effective decrease in protein adsorption.

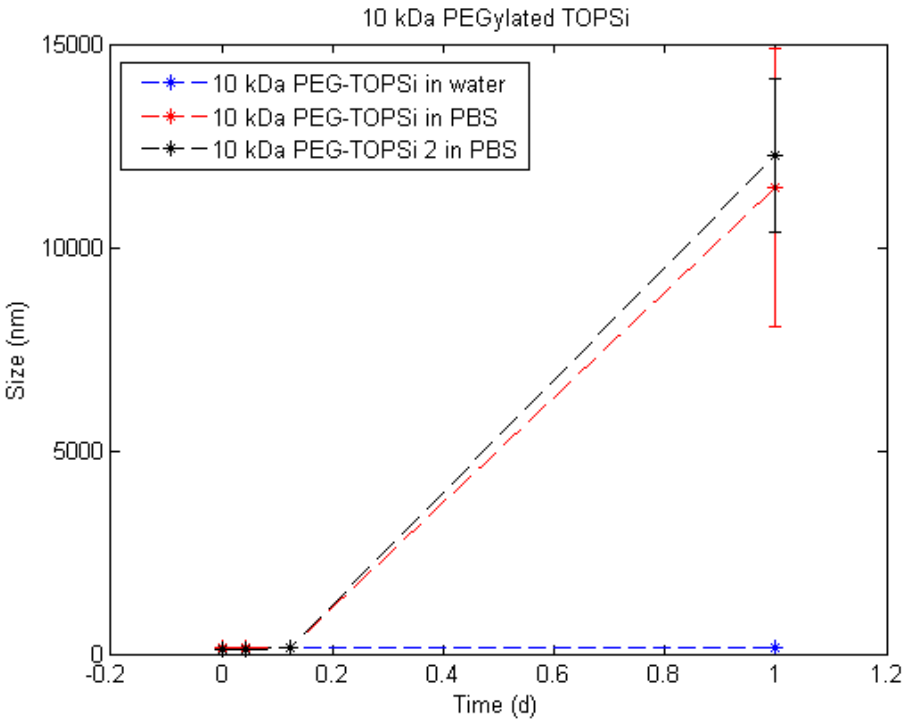

Figure 26: Stability of 10 kDa PEG-TOPSi in H_2O and PBS.

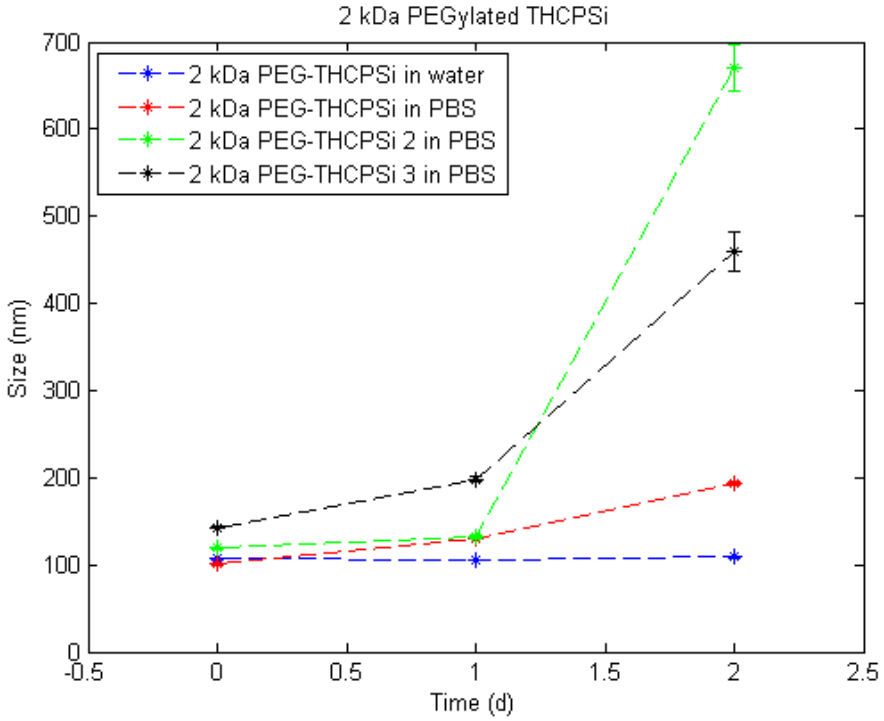

Figure 27: Stability of 2 kDa PEG-THCPSi in H_2O and PBS.

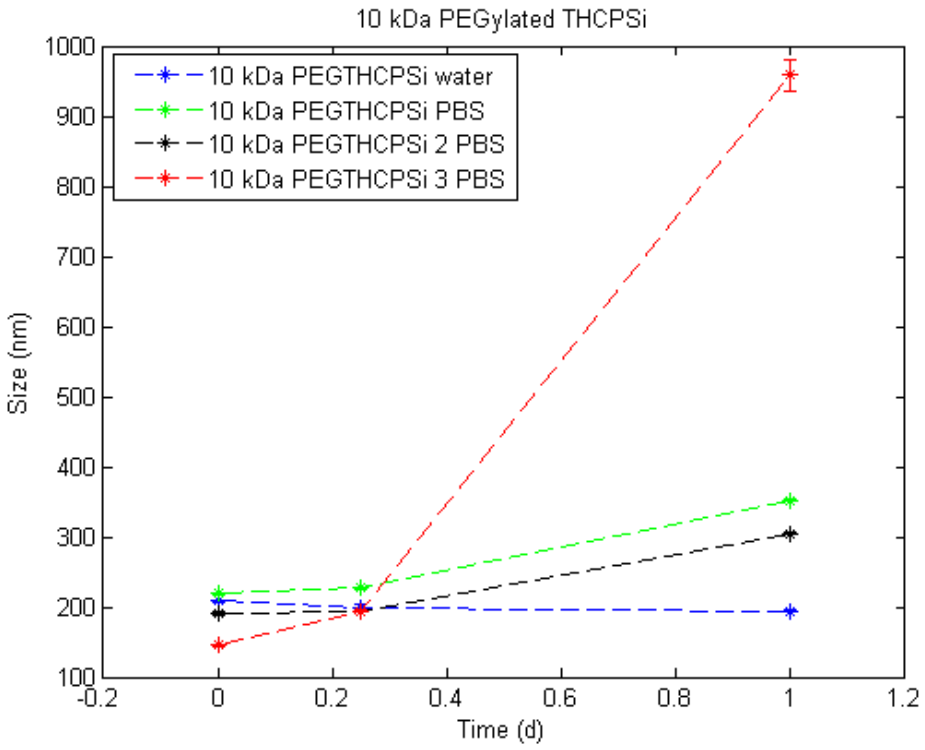

Figure 28: Stability of 10 kDa PEG-THCPSi in H_2O and PBS.

Storm et al. [83] reported that the coating thickness should be at least 5 % of particle diameter to prevent aggregation. This result would give us explanation to why 0.5 kDa PEG did not work but no idea why 10 kDa did not work. While the reason why 10 kDa PEGlation did not work is still unclear, the used method seemed suitable for 2 kDa PEGylation.

To verify these results, also THCPSi-OH particles were PEGylated with 2 kDa PEG and for comparison with 10 kDa PEG. The results are shown in Fig. 27 for 2 kDa PEG-THCPSi and Fig. 28 for 10 kDa PEG-THCPSi.

With 2 kDa PEGylated THCPSi the results were worse than expected as particles aggregated after one day. For 10 kDa PEGylated however the results seem to be better than with 10 kDa TOPSi as particles did not aggregate that strongly. The reason for both of these could be the amount of hydroxyl groups which are utilized in attaching PEG molecules to the surface. As the hydroxyl group amount might be lower in THCPSi-OH than in TOPSi-OH, the attached 2 kDa PEG surface density might have decreased below the critical wt% needed to prevent aggregation. With 10 kDa the grafting density may have decreased a bit to allow better mobility for PEG chains which resulted in slightly better colloidal stability.

As 2 kDa PEG-TOPSi gave best results, its usage in further *in vivo* tests were considered. For these tests it would be important to be able to track the particle circulation. For this purposes either APTES or Triethoxy(4-methoxyphenyl) silane (later on referred as Phenyl) was grafted to the surface of PEGylated TOPSi particles. The idea was that these molecules could be radiolabelled with radioactive iodine which could be tracked on the *in vivo* tests.

However when trying to make 2 kDa PEG-TOPSi material it was found that the material made wasn't stable. While repeating the process for manufacturing the 2 kDa TOPSi particles it came clear that drying of the solvent in the process is very crucial. After this was figured out the manufacture of 2 kDa PEG-TOPSi was found again successful and the APTES/Phenyl attachment studies could be continued.

The amount of APTES or Phenyl was kept to minimun to prevent aggregation. However, no matter how low amount of APTES or Phenyl was used in grafting reaction, the results showed aggregation (Fig. 29 and Fig. 30). The NH_2 modified particles showed faster aggregation than Phenyl modified which is mostly due the positive surface charge it haves. The Z-potential of PEGylated TOPSi particles were -8 mV (in water) whereas NH_2 grafted PEG-TOPSi particles had Z-potential of +30 mV (in water). While higher Z-potential should lead to better stability it seems that NH_2 molecules interferes the abilities of PEG. Also Phenyl molecules seem to interefere PEG molecules but not as much as NH_2 as their stability is slightly better.

Even though aggregation was seen, the effect of PEGylation is clear. The uncoated NH_2-TOPSi and Phenyl-TOPSi aggregate fastly within hours (results not shown) where as PEGylated particles showed slower aggregation.

It is reported that shorter PEGs tend to form brush-like coating and longer PEGs mushroom-like layer [19]. Both layer types have their own advantages and disadvantages [83]. It was assumed that combining two different size of PEG would be more efficient in preventing aggregation. This was assumed to be due the possibility to have both brush-like and mushroom-like layers on the surface of particle. To investigate this, the TOPSi-OH particles were simultaneously PEGylated with 0.5 kDa and 2 kDa PEG.

The results showed, quite luckily even, that PEGylation with two different sizes PEG resulted in stable particles (Fig. 31). These 2+0.5 kDa PEGylated TOPSi particles remained stable for the whole measurement time. The improvement compared to only 2 kDa PEG-TOPSi were obvious as no aggregation were seen.

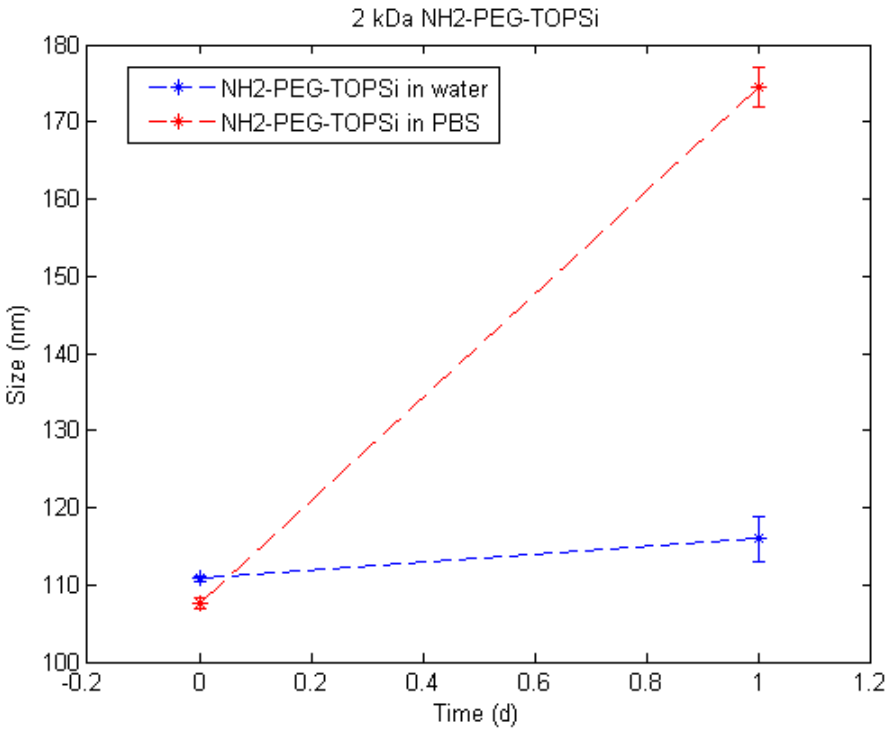

Figure 29: Stability of 2 kDa NH_2-PEG-TOPSi in H_2O and PBS.

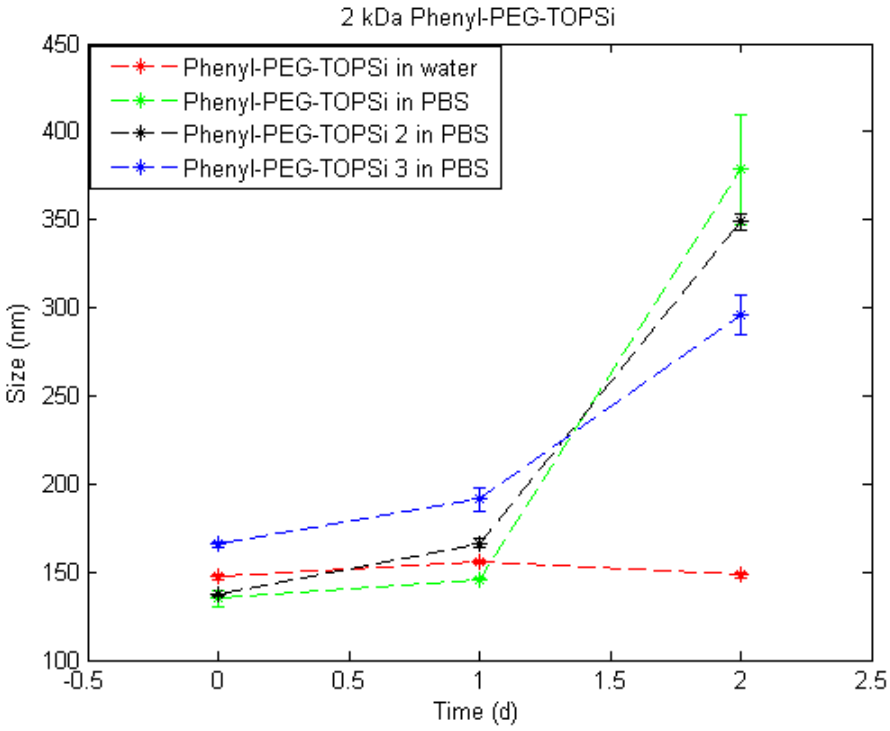

Figure 30: Stability of 2 kDa Phenyl-PEG-TOPSi in H_2O and PBS.

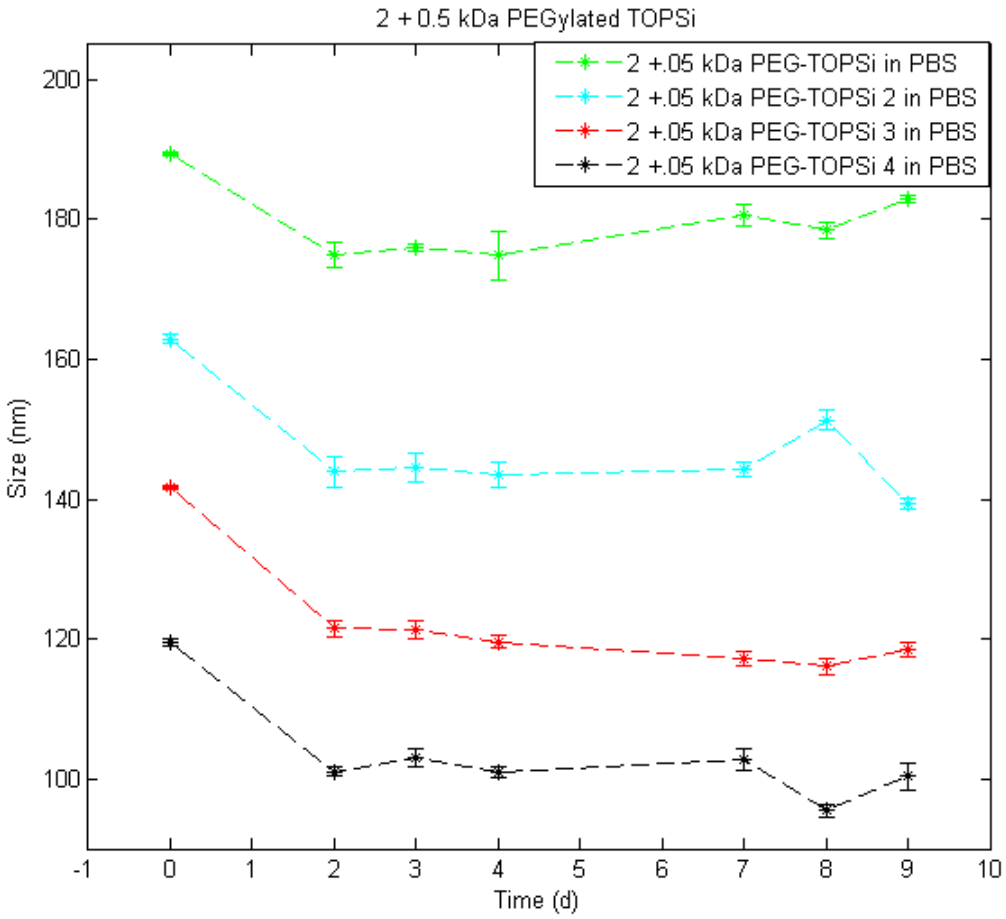

Figure 31: Stability of 2+0.5 kDa PEG-TOPSi in PBS.

Worth mentioning is that now also the bigger particles were stable (compared to Fig. 25). Between the first two time points a size decrease was observed in all the sizes. This is most like due the mushroom-like layer forming to the surface of the particle. The 0.5 kDa PEG layer is most likely reason for this effect as it wasn't seen on just 2 kDa PEGylation or at least the effect is now slowed and therefore it is seen on measurements.

Depending on the reason, the underlying 0.5 kDa layer might induce energetically favoured space for 2 kDa PEG to fold into. The other, and more possible, reason might be that the 0.5 kDa brush-like layer is preventing the upper 2 kDa layer from folding into tight mushroom cloud. The folding 2 kDa PEG chains might bounce off from the 0.5 kDa layer which will try to prevent bending and induce counter force towards 2 kDa PEG chains similarly as in case of protein adsorpion.

The final state, where 2 kDa PEG might fold to, would therefore be a bit above the 0.5 kDa layer. The size decrease seen on Fig. 31 would reinforce this theory. The size decreases seen were about 20 nm, meaning decrease of 10 nm at each size of the particle. As the lengths of 2 kDa and 0.5 kDa PEG are, respectively, 15,8 nm and 3.9 nm, the 2 kDa layer seem to form about 2 nm above the 0.5 kDa brush-like layer.

This would also explain better stability of 2+0.5 kDa particles. As particles try to get closer each other the upper (2 kDa) layer will bend and form a counter force towards the particle. As particles get closer to each other, the 0.5 kDa layer also starts to bend. This layer similarly forms a counter force that, with the counter force of 2 kDa layer, is strong enough for preventing aggregation. For these particles there was also more PEG molecules at the surface (20 wt%, results not shown). The better stability might partly be due the better surface coating resulted in 2+0.5 kDa PEGylation.

During these measurement the color change of measured dispersion was seen. This was concluded to be due dissolution of porous silicon. In lack of better equipment the dissolution of porous silicon was monitored with DLS. From the size measurements one can get count rate of each measurement which is proportional to the particle amounts. The decrease of count rates was obvious in every sample that was in PBS (Fig. 32). In water however the particles seemed to be stable. By using count rates, the silicon amount (%) in the samples were calculated (Fig. 33). The dissolution of silicon could be seen clearly from the measurement vials during the measurement (Fig. 34).

The dissolution of porous silicon is not new thing but the time range where it happened suprised a bit. The discovery was actually quite beneficial as dissolution of PSi is wanted for drug delivery applications. As PSi would dissolve spontaneously in the body, it could be more easily excreted from the body and therefore would not cause any toxic effects. PEGylation actually seems to have positive effect on PSi life time. There are studies that report complete dissolution of PSi in 8h [95] for particles incubated in PBS at 37 °C.

Compared to reported values, the PEGylation improves the stability of PSi a lot. The dissolution experiments done to 2 kDa PEG-TOPSi particles also gave better life times (results not shown) as reported results [95]. However the life time of 2 kDa PEG-TOPSi particles were shorter than with 2+0.5 kDa PEG-TOPSi particles. These results indicate that manufactured 2+0.5 PEG-TOPSi particles would be very suitable for *in vivo* experiments.

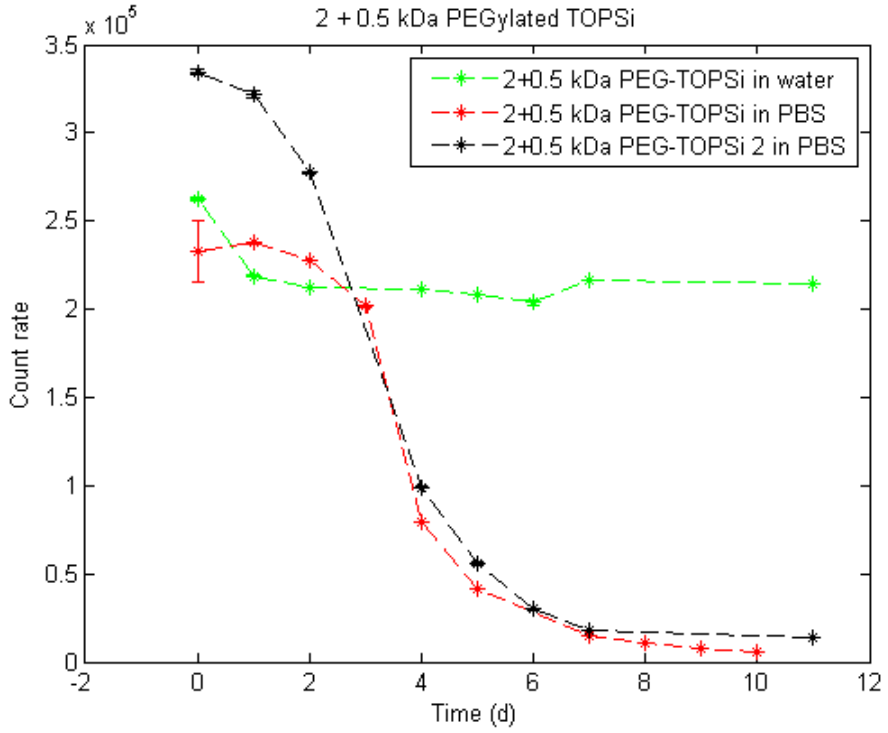

Figure 32: The count rates of 2+0.5 kDa PEG-TOPSi samples in PBS and H_2O.

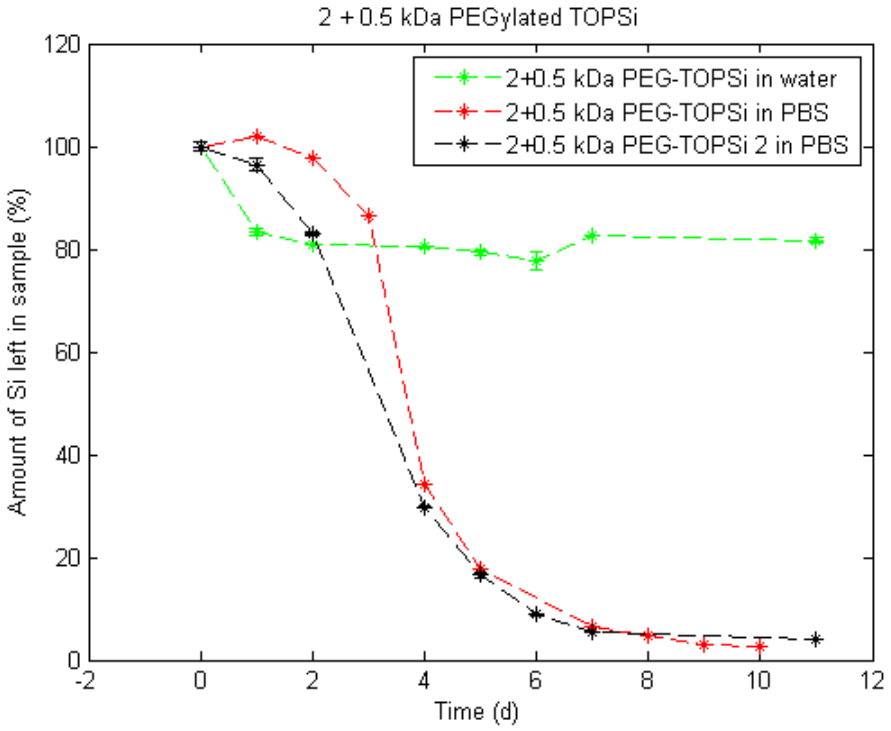

Figure 33: The amount of Si in 2+0.5 kDa PEG-TOPSi samples in PBS and H_2O.

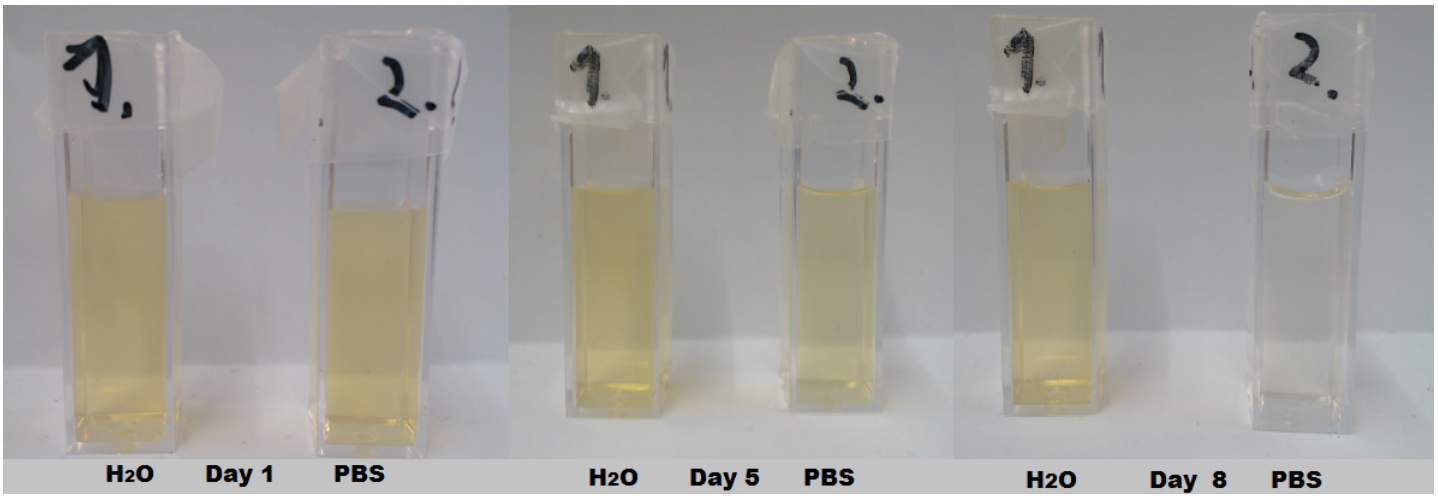

Figure 34: The dissolution of 2+0.5 PEG-TOPSi seen from measurement vials during the experiment. The vials numbered 1 are dispersed in water and vials numbered 2 are dispersed in PBS.

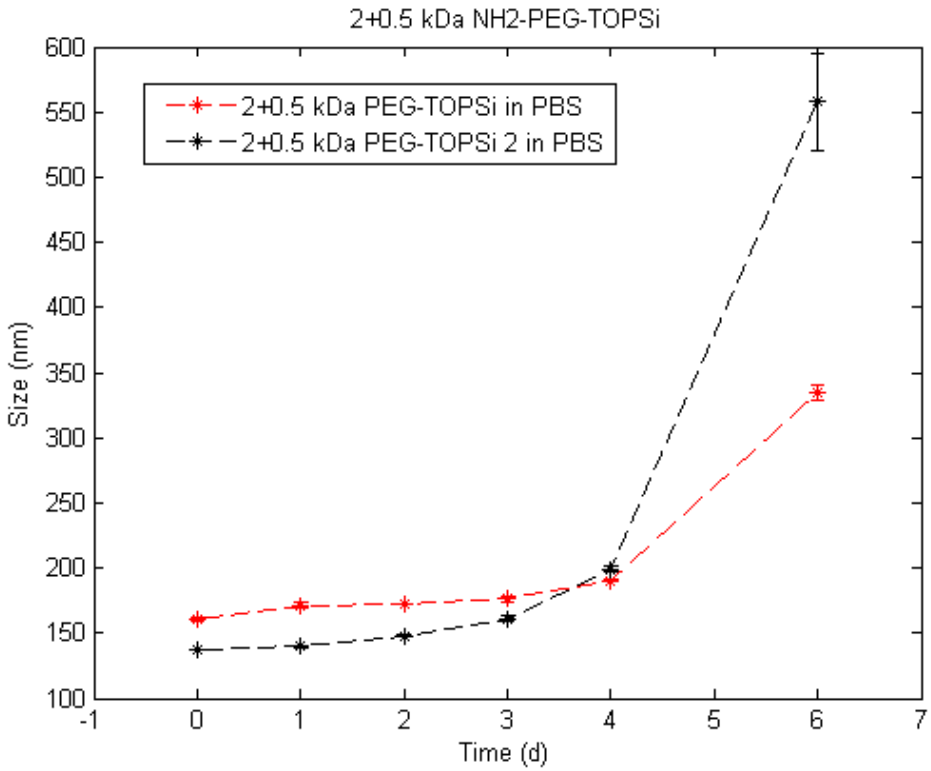

Figure 35: Stability of 2+0.5 kDa NH_2-PEG-TOPSi in PBS.

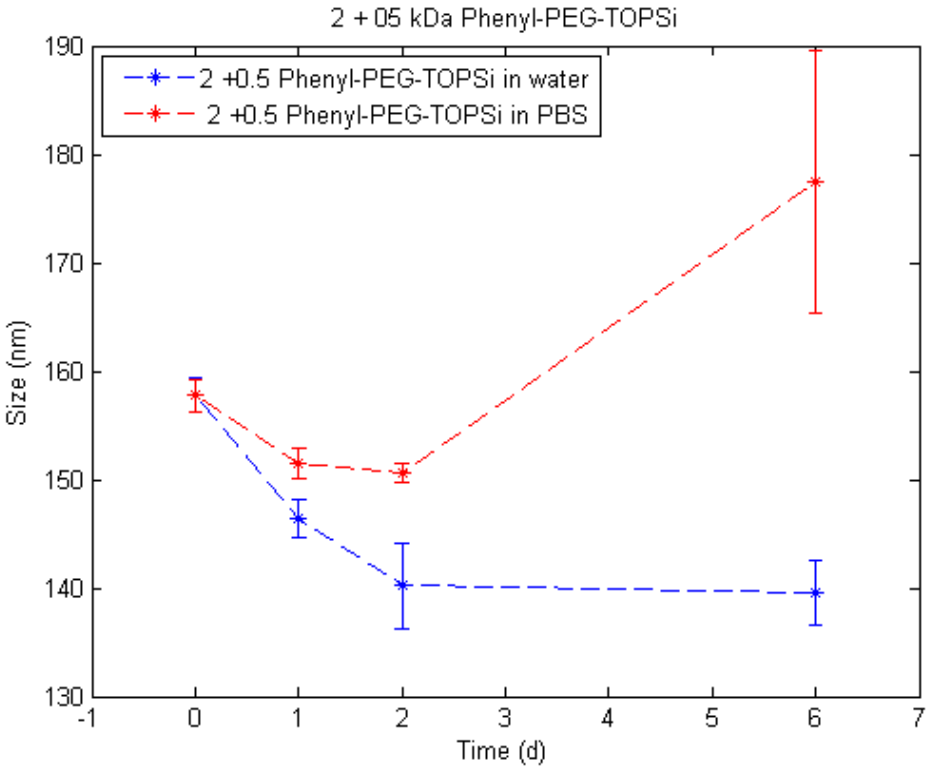

Figure 36: Stability of 2+0.5 kDa Phenyl-PEG-TOPSi in PBS.

For tracking the particles at *in vivo* test the NH_2 and Phenyl grafting was again tried. Now the results were much more promising as both NH_2-PEG-TOPSi and Phenyl-PEG-TOPSi particles showed improved stability (Fig. 35 and Fig. 36). With the 2+0.5 kDa PEGylation the stability of NH_2-PEG-TOPSi and Phenyl-PEG-TOPSi increased up to 4 and 2 days, respectively. The stability of Phenyl-PEG-TOPSi might be similar to NH_2-PEG-TOPSi particles but this cannot be proven as the author had force majeure and could not measure the Phenyl-PEG-TOPSi samples as frequently as he wanted.

5.3 Conclusions

The results clearly indicate that with the successful PEGylation the particle colloidal stability can be improved. With the best, 2+0.5 kDa PEG-TOPSi, particles, the samples were stable for up to 9 days in PBS. At this time the particle dissolution was also observed. The dissolution, once it has been initiated, seems to happen very rapidly as the particle size stays stable and there are no evidence of smaller particles.

pH might be the reason why PEGylated TOPSi particles did not totally dissolve in water. As PBS keeps same pH over the whole measurement, the dissolution can continue and silicon can be totally dissolved. With water, as some dissolution occurs the pH might drop because of the silicic acid. This pH drop causes that silicon dissolution is no longer favorable and the silicon particles have long life time in water. The study done Anderson et al. [64] reinforce this hypothesis as they saw dissolution of PSi to diminish to zero as the pH was decreased. The reason for dissolution and its mechanism need however more investigations.

The reason why only 2 kDa and 2+0.5 kDa PEGylations were successful is unclear. The reason migth be in grafting densities which weren't appropriate for 0.5 kDa and 10 kDa PEGylations. These particles might have had too sparse or too dense coatings which did not result in positive results. It seems that the process used here was optimal for 2 kDa PEG since we did not alter the PEG molecule amount in the PEGylation process at any point. In future it should be studied whether the grafting densities really are the reason for differences in colloidal stability. Nonetheless it seems that in 2 kDa PEGylated particles the polymer chains maintain their mobility and flexibility which is crucial for preventing aggregation and protein adsorption.

The adding of smaller PEG seems to strengthen these effects and results in even more stable particles. Reason behind this might be due to better coating that can be achieved with two different PEG sizes at the surface. Another explanation is the existence of two different PEG conformations (brush- and mushroom-like) which together provide better prevention against aggregation.

The evaporation of process solvent seems critical for successful PEGylation. The reason behind this might be the increasing concentration of PEG molecules as the solvent is evaporating which might result in better coating. Also as solvent is evaporated the PEG molecules might drift closer to the surface and more PEG molecules can be attached. This wasn't studied in this thesis and so in future it should be tested e.g. with TG if the evaporation increases the amount of PEG (wt%) on the particles.

While the reasons might be very complex it is clear that PEGylation can prevent aggregation very efficiently. This was seen also with APTES and Phenyl modified 2+0.5 kDa PEG-TOPSi which showed improved colloidal stability. With these improvements the particles modified with APTES or Phenyl could be used on *in vivo* tracking.

The manufactured 2+0.5 kDa PEG-TOPSi particles seem very stable and promising to be used in further applications. However as tests were only done in PBS the next step it to make stability testing in blood plasma. Also the effect of PEG surface density should be studied as well as the protein adsorption before and after PEGylation. A big question is where the PEG is attaching; it might be attaching to the pore walls which is undesired. To study this phenomenon the particles could be measured with DSC (differential scanning calorimetry). DSC might be able to detect the different attachment points of PEG as the desorbing temperatures should differ between PEG molecules on the surface on the pores.

With all this said it is clear that the PEGylation needs still a lot more studying. These include studying the attachment point, the effect of grafting density and PEG length on colloidal stability and the effect of solvent evaporation. Also as next step, the *in vitro* colloidal stability tests should be done in plasma and the protein adsorption should be also studied. If these studies are successful then the logical step is to move into *in vivo* tests.

Nonetheless the results of this thesis cannot be ignored as the colloidal stability was seen to increase up to 9 days whereas it was under one day for plain particles.

References

[1] A. Uhlir Jr., Electrolytic shaping of germanium and silicon, *Bell Syst. Tech.*, J., **35**, pp. 333-347, 1956.

[2] D. R. Turner, Electropolishing Silicon in Hydrofluoric Acid Solutions, *J. Electrochem. Soc.*, **105** (7), pp. 402-408, 1958.

[3] R. Memming and G. Schwandt, Anodic dissolution of silicon in hydrofluoric acid solutions, *Surf. Sci.*, **4** (2), pp. 109-124, 1966.

[4] L. T. Canham, Silicon quantum wire array fabrication by electrochemical and chemical dissolution of wafers, *Appl. Phys. Lett.*, **57** (10), pp. 1046-1048, 1990.

[5] L. T. Canham, Bioactive silicon structure fabrication through nanoetching techniques, *Adv. Mater.*, **7** (12), pp. 1033-1037, 1995.

[6] J. Salonen, L. Laitinen, A. M. Kaukonen, J. Tuura, M. Björkqvist, T. Heikkilä, K. Vähä-Heikkilä, J. Hirvonen, V.-P. Lehto, Mesoporous silicon microparticles for oral drug delivery: Loading and release of five model drugs, *J. Control. Release*, **108** (2-3), pp. 362-374, 2005.

[7] J. Riikonen, E. Mäkilä, J. Salonen and V. -P. Lehto, Determination of the Physical State of Drug Molecules in Mesoporous Silicon with Different Surface Chemistries, *Langmuir*, **25** (11), pp. 6137-6142, 2009.

[8] E. Tasciotti, X. Liu, R. Bhavane, K. Plant, A. D. Leonard, B. K. Price, M. M. - C. Cheng, P. Decuzzi, J. M. Tour, F. Robertson and M. Ferrari, Mesoporous silicon particles as a multistage delivery system for imaging and therapeutic applications, *Nat. Nanotechnol.*, **3**, pp. 151 - 157, 2008.

[9] A. S. Goh, A. Y. Chung, R. H. Lo, T. N. Lau, S. W. Yu, M. Chng, S. Satchithanantham, S. L. Loong, D. C. Ng, B. C. Lim, S. Connor & P. K. Chow, A novel approach to brachytherapy in hepatocellular carcinoma using a phosphorous32 (^{32}P) brachytherapy delivery device–a first-in-man study, *Int. J. Radiat. Oncol. Biol. Phys.*, **67** (3), pp. 786-792, 2007.

[10] E. J. Anglin, L. Cheng, W. R. Freeman and M. J. Sailor, Porous silicon in drug delivery devices and materials, *Advanced Drug Delivery Reviews*, **60** (11), pp. 1266-1277, 2008.

[11] L. M. Bimbo, E. Mäkilä, T. Laaksonen, V. -P. Lehto, J. Salonen, J. Hirvonen and H. A. Santos, Drug permeation across intestinal epithelial cells using porous silicon nanoparticles, *Biomaterials*, **32** (10), pp. 2625-2633, 2011.

[12] H. Maeda, J. Wu, T. Sawa, Y. Matsumura and K. Horic, Tumor vascular permeability and the EPR effect in macromolecular therapeutics: a review, *J. Control. Release*, **65** (1-2), pp. 271-284, 2000.

[13] R. B. Vasani, S. J. P. McInnes, M. A. Cole, A. M. Md Jani, A. V. Ellis and N. H. Voelcker, Stimulus-Responsiveness and Drug Release from Porous Silicon Films ATRP-Grafted with Poly(N-isopropylacrylamide), *Langmuir*, **27** (12), pp. 7843-7853, 2011.

[14] R. Y. Hong, B. Feng, L. L. Chen, G. H. Liu, H. Z. Li, Y. Zheng and D. G.Wei, Synthesis, characterization and MRI application of dextran-coated Fe3O4 magnetic nanoparticles, *Biochem. Eng. J.*, **42** (3), pp. 290-300, 2008.

[15] J. V. Jokerst, T. Lobovkina, R. N. Zare and S. S. Gambhir, Nanoparticle PEGylation for imaging and therapy, *Nanomedicine*, **6** (4), pp. 715-728, 2011.

[16] M. Kim, J. Jung, J. Lee, K. Na, S. Park adn J. Hyun, Amphilic comblike polymers enhance the colloidal stability of Fe_3O_4 nanoparticles, *Colloids Surf. B Biointerfaces*, **76** (1), pp. 236-240, 2010.

[17] C. Fang, B. Shi, Y. -Y. Pei, M. -H. Hong, J. Wub and H. -Z. Chen, In vivo tumor targeting of tumor necrosis factor-α-loaded stealth nanoparticles: Effect of MePEG molecular weight and particle size, *Eur. J. Pharm. Sci.*, **27** (1), pp. 27-36, 2006.

[18] R. Gref, Y. Minamitake, M. T. Peracchia, V. Trubetskoy, V. Torchilin and R. Langer, Biodegradable Long-Circulating Polymeric Nanospehers, *Science*, **263** (5153), pp. 1600-1603, 1994.

[19] Z. Yang. J. A. Galloway and H. Yu, Protein Interactions with Poly(ethylene glycol) Self-Assembled Monolayers on Glass Substrates: Diffusion and Absorption, *Langmuir*, **15** (23), pp. 8405-8411, 1999.

[20] S. J. Sofia, V. Premnath and E. W. Merril, Poly(ethylene oxide) Grafted to Silicon Surfaces: Grafting Density and Protein Adsorption, *Macromolecules*, **31**, pp. 5059-5070, 1998.

[21] E. Ostuni, R. G. Chapman, R. E. Holmlin, S. Takayama and G. M. Whitesides, A Survey of Structure- Property Relationships of Surfaces that Resist the dtion of Protein, *Langmuir*, **17** (18), pp. 5605-5620, 2001.

[22] R. Gref, M. Lück, P. Quellec, M. Marchand, E. Dellacherie, S. Harnisch, T. Blunk and R. H. Müller, 'Stealth' corona-core nanoparticles surface modified by polyethylene glycol (PEG): influences of the corona (PEG chain length and surface density) and the core composition on phagocytic uptake and plasma protein adsorption, *Colloids Surf. B Biointerfaces*, **18** (3-4), pp. 301-313, 2000.

[23] J. L. Coffer, Porous silicon formation by stain etching, in *Properties of Porous Silicon*, **18**, (ed. L. T. Canham), Institution of Engineering and Techology, London, pp. 23-29, 1997.

[24] C. H. Choy and K. W. Cheah, Laser-induced etching of silicon, *Appl. Phys. A*, **61** (1), pp. 45-50, 1995.

[25] A. Halimaoui, Porous silicon formation by anodisation, in *Properties of Porous Silicon*, **18**, (ed. L. T. Canham), Institution of Engineering and Techology, London, pp. 12-22, 1997.

[26] G. Korotcenkov and B. K. Cho, Silicon porosification: State of the Art, *Critical Reviews in Solid State and Material Sciences*, **35** (3), pp. 153-260, 2011.

[27] J. Salonen, A. M. Kaukonen, J. Hirvonen and V. -P. Lehto, Mesoporous Silicon in Drug Delivery Applications, *J. Pharm. Sci.*, **97** (2), pp. 632-653, 2008.

[28] X. G. Zhang, S. D. Collins and R. L. Smith, Porous Silicon Formation and Electropolishing of Silicon by Anodic Polarization in HF Solution, *J. Electrochem. Soc.*, **136** (5), pp. 1561-1565, 1989.

[29] V. Lehmann, The physics of macropore formation in low doped n-type silicon, *J. Electrochem. Soc.*, **140** (10), pp. 2836-2843, 1993.

[30] V. Lehmann, R. Stengl, A. Luigart, On the morphology and the electrochemical formation mechanism of mesoporous silicon, *Materials Science and Engineering B* **69-70**, pp. 11-22, 2000.

[31] H. Föll, J. Cartensen and S. Frey, Porous and Nanoporous Semiconductors and Emerging Applications, *J. Nanomater.*, **2006**, 91635, 2006 .

[32] A. Yu. Panarin, S. N. Terekhov, K. I. Kholostov and V. P. Bondarenko, SERS-active substrates based on n-type porous silicon, *Appl. Surf. Sci.*, **256** (23), pp. 6969-6976, 2010.

[33] K. Rumpf, P. Granitzer, P. Poelt and H. Krenn, Transition metals specifically electrodeposited into porous silicon, *Phys. Stat. Sol.*, **6** (7), pp. 1592-1595, 2009.

[34] O. Bisia, Stefano Ossicinib, L. Pavesi, Porous silicon: a quantum sponge structure for silicon based optoelectronics, *Surf. Sci. Rep.* **38** (1), pp. 1-126, 2000.

[35] D. Bellet, Drying of porous silicon, in *Properties of Porous Silicon*, **18**, (ed. L. T. Canham), Institution of Engineering and Techology, London, pp. 38-43, 1997.

[36] J. -N. Chazaviel and F. Ozanam, Surface modification of porous silicon, in *Properties of Porous Silicon*, **18**, (ed. L. T. Canham), Institution of Engineering and Techology, London, pp. 59-65, 1997.

[37] J. -N. Chazaviel, R. B. Wehrspohn and F. Ozanam, Electrochemical preparation of porous semiconductors: from phenomenology to understanding, *Mater. Sci. Eng. B*, **69-70**, pp. 1-10, 2000.

[38] K. W. Kolasinski, Etching of silicon in fluoride solutions, *Surf. Sci.*, **603**, (10-12), pp. 1904-1911, 2009.

[39] K. W. Kolasinski, The mechanism of Si etching in fluoride solutions, *Phys. Chem. Chem. Phys.*, **5**, pp. 1270-1278, 2003.

[40] E. S. Kooij and D. Vanmaekelbergh, Catalysis and Pore Initiation in the Anodic Dissolution of Silicon in HF, *J. Electrochem. Soc.* , **144** (4), pp. 1296-1301, 1997.

[41] V. Lehmann and U. Gosele, Porous silicon formation: A quantum wire effect, *Appl. Phys. Lett.*, **58** (8), pp. 856-858, 1991.

[42] J. Salonen, V. -P. Lehto and E. Laine, Thermal oxidation of free-standing porous silicon films, *Appl. Phys. Lett.*, **70** (5), pp. 637-639, 1997.

[43] W. Xu, J. Riikonen, T. Nissinen, M. Suvanto, K. Rilla, B. Li, Q. Wang, F. Deng and V. -P. Lehto, Amine Surface Modifications and Fluorescent Labeling of Thermally Stabilized Mesoporous Silicon Nanoparticles, *J. Phys. Chem. C*, **116** (42), pp. 22307-22314, 2012.

[44] V. Usković, P. P. Lee, L. A. Walsh, K. E. Fischer and T. A. Desai, PEGylated silicon nanowire coated silica microparticles for drug delivery across intestinal epithelium, *Biomaterials*, **33** (5), pp. 1663-1672, 2012.

[45] T. Strother, W. Cai, X. Zhao, R. J. Hamers and L. M. Smith, Synthesis and Characterization of DNA-Modified Silicon (111) Surfaces, *J. Am. Chem. Soc.* **122** (6), pp. 1205-1209, 2000.

[46] B. R. Hart, S. E. Letant, S. R. Kane, M. Z. Hadi, S. J. Shields, and J. G. Reynolds, New method for attachment of biomolecules to porous silicon, *Chem. Commun.* **3**, pp. 322-323, 2003.

[47] M. Arroyo-Hernández, R. J. Martín-Palma, J. Pérez-Rigueiro, J. P. García-Ruiz, J. L. García-Fierro and J. M. Martínez-Duart, Biofunctionalization of surfaces of nanostructured porous silicon, *Material Science and Engineering C*, **23** (6-8), pp. 697-701, 2003.

[48] D. Gallach, G. Recio-Sáchez, A. Múnoz-Noval, M. Manso-Silván, G. Ceccone, R. J. Martín-Palma, V. Torres-Costa and J. M. Martínez-Duart, Functionality of porous silicon particles: Surface modification for biomedical applications, *Materials Science and Engineering: B*, **169** (1-3), pp. 123-127, 2010.

[49] T. Tanaka, L. S. Mangala, P. E. Vivas-Mejia, R. Nieves-Alicea, A. P. Mann, E. Mora, H. D. Han, M. M. Shahzad, X. Liu, R. Bhavane, J. Gu, J. R. Fakhoury, C. Chiappini, C. Lu, K. Matsuo, B. Godin, R. L. Stone, A. M. Nick, G. Lopez-Berestein, A. K. Sood and M. Ferrari, Sustained small interfering RNA delivery by mesoporous silicon particles, *Cancer Res.*, **70** (9), pp. 3687-3796, 2010.

[50] K. L. Prime and G. M. Whitesides, Self-Assembled Organic Monolayers: Model Systems for Studying Adsorption of Proteins at Surfaces, *Science*, **252** (5009), pp. 1164-1167, 1991.

[51] B. A. Kairdolf, M. C. Mancini, A. M. Smith and S. Nie, Minimizing Nonspecific Cellular Binding of Quantum Dots with Hydroxyl-Derivatized Surface Coatings, *Anal. Chem.*, **80** (8), pp. 3029-3034, 2008.

[52] M. P. Schwartz, F. Cunin, R. W. Cheung and M. Sailor, Chemical modification of silicon surfaces for biological applications, *Phys. Stat. Sol. (a)*, **202** (8), pp. 1380-1384, 2005.

[53] A. Papra, N. Gadegaard and N. B. Larsen, Characterization of Ultrathin Poly(ethylene glycol) Monolayers on Silicon Substrates, *Langmuir*, **17** (5), pp. 1457-1460, 2001.

[54] O. Tabasi, C. Falamaki and Z. Khalaj, Functionalized mesoporous silicon for targeted-drug-delivery, *Colloids and Surfaces B: Biointerfaces*, **98**, pp. 18-25, 2012.

[55] J. F. Stefanick, J. D. Ashley, T. Kiziltepe and B. Bilgicer, A systematic Analysis of Peptide Linker Length and Liposomal Polyethylene Glycol Coation on Cellular Uptake of Peptide-Targeted Liposomes, *ACS Nano*, **7** (4), pp. 2935-2947, 2013.

[56] K. Miyata, N. Nishiyama and K. Kataoka, Rational design of smart supramolecular assemblies for gene delivery:chemical challenges in the creation of artificial viruses, *Chem. Soc. Rev.*, **41** (7), pp. 2562-2574, 2012.

[57] F. Alexis, E. Pridgen, L. K. Molnar and O. C. Farokzad, Factors Affecting Clearance and Biodistribution of Polymeric Nanoparticles, *Mol. Pharmaceutics*, **5** (4), pp. 505-515, 2008.

[58] M. Benezra, O. Penate-Medina, P. B. Zanzonico, D. Schaer, H. Ow, A. Burns, E. DeStanchina, V. Longo, E. Herz, S. Iyer, J. Wolchok, S. M. Larson, U. Wiesner and M. S. Bradbury, Multimodal silica nanoparticles are effective cancer-targeted probes in a model of human melanoma, *J. Clin. Invest.*, **121** (7), pp. 2768-2780, 2011.

[59] B. D. Ratner, Reducing capsular thickness and enhancing angiogenesis around implant drug release systems, *J. Controlled Release*, **78** (1-3), pp. 211-218, 2002.

[60] D. F. Williams, Definitions in Biomaterials, *Progress in Biomedical Engineering*, **4**, 1987.

[61] D. F. Williams, On the mechanisms of biocompatibility, *Biomaterials*, **29** (20), pp. 2941-2953, 2008.

[62] L. T. Canham, J. P. Newey, C. L. Reeves, M. R. Houlton, A. Loni, A. J. Simons and T. I. Cox,The Effects of DC Electric Currents on the In-Vitro Calcification of Bioactive Silicon Wafers, *Adv. Mater.*, **8** (10), pp. 847-849, 1996.

[63] S. P. Low, N. H. Voelcker, L. T. Canham and K. A. Williams, The biocompatibility of porous silicon in tissues of the eye, *Biomaterials*, **30** (15), pp. 2872-2880, 2009.

[64] S. H. C. Anderson, H. Elliott, D. J. Wallis, L. T. Canham and J. J. Powell,Dissolution of different forms of partially porous silicon wafers under simulated physiological conditions, *Phys. Stat. Sol. (a)*, **197** (2), pp. 331-335, 2003.

[65] S. C. Bayliss, R. Heald, D. I. Fletcher and L. D. Buckberry, The Culture of Mammalian Cells on Nanostructured Silicon, *Adv. Mater.*, **11** (4), pp. 318-321, 1999.

[66] R. Jugdaohsingh, K. L Tucker, N. Qiao, L. A. Cupples, D. P. Kiel and J. J. Powell, Dietary Silicon Intake Is Positively Associated With Bone Mineral Density in Men and Premenopausal Women of the Framingham Offspring Cohort, *J. Bone Miner. Res.*, **19** (2), pp. 297-307, 2004.

[67] C. Hong and C. Lee, In vitro cell tests of pancreatic malignant tumor cells by photothermotherapy based on DMSO porous silicon colloids, *Lasers Med. Sci.*, 2013.

[68] D. -E. Lee, H. Koo, I. -C. Sun, J. H. Ryu, K. Kim and I. C. Kwon, Multifunctional nanoparticles for multimodal imaging and theragnosis, *Chem. Soc. Rev.*, **41** (7), pp. 2656-2672, 2012.

[69] N. Lee and T. Hyeon, Designed synthesis of uniformly sized iron oxide nanoparticles for efficient magnetic resonance contrast agents, *Chem. Soc. Rev.*, **41**, pp. 2575-2589, 2012.

[70] D. E Owens III and N. A. Peppas, Opsonization, biodistribution, and pharmacokinetics of polymeric nanoparticles, *International Journal of Pharmaceutics*, **307** (1), pp. 93-102, 2006.

[71] K. Knop, R. Hoogenboom, D. Fischer and U. S. Schubert, Poly(ethylene glycol) in Drug Delivery: Pros and Cons as Well as Potential Alternatives, *Angew. Chem. Int. Ed.*, **49** (36), pp. 6288-6308, 2010.

[72] M. Roser, D. Fischer and T. Kissel, Surface-modified biodegradable albumin nano- and microspheres. II: effect of surface charges on in vitro phagocytosis and biodistribution in rats, *Eur. J. Pharm. Biopharm.*, **46** (3), pp. 255-263, 1998.

[73] Z. Li, J. C. Barnes, A. Bosoy, J. F. Stoddart and J. I. Zink, Mesoporous silica nanoparticles in biomedical applications, *Chem. Soc. Rev.*, **41** (7), pp. 2590-2605, 2012.

[74] J. S. Souris, C. -H. Lee, S. -H. Cheng, C. -T. Chen, C. -S. Yang, J. A. Ho, C. -Y. Mou and L. -W. Lo, Surface charge-mediated rapid hepatobiliary excretion of mesoporous silica nanoparticles, *Biomaterials*, **31** (21), pp. 5564-5574, 2010.

[75] R. E. Holmlin, X. Chen, R.G. Champman, S. Takayama and G. M. Whitesides, Zwitterionic SAMs that Resist Nonspecific Adsorption of Prorein from Aqueous Buffer, *Langmuir*, **17** (9), pp. 2841-2850, 2001.

[76] C. -H. Lee, S. -H. Cheng, Y. -J. Wang, Y. -C. Chen, N. -T. Chen, J. Souris, C. -T. Chen, C. -Y. Mou, C. -S Yang and L. -W Lo, Near-Infrared Mesoporous Silica Nanoparticles for Optical Imaging: Characterization and In Vivo Biodistribution, *Adv. Funct. Mater.*, **19** (2), pp. 215-222, 2009.

[77] S. -H. Wu, Y. -S. Lin, Y. Hung, Y. -H. Chou, Y. -H. Hsu, C. Chang and C. -Y. Mou, Multifunctional Mesoporous Silica Nanoparticles for Intracellular Labeling and Animal Magnetic Resonance Imaging Studies, *Chembiochem*, **9** (1), pp. 53-57, 2008.

[78] S. H. Vakili Tahami, Z. Ranjbar and S. Bastani, Aggregation and Charging Behavior of Polydisperse and Monodisperse Colloidal Epoxy-Amine Adducts, *Soft Material*, **11** (3), pp. 334-345, 2013.

[79] C. Shen, F. Wang, B. Li, Y. Jin, L. - P. Wang and Y. Huang, Application of DLVO Energy Map To Evaluate Interactions between Spherical Colloids and Rough Surfaces, *Langmuir*, **28** (41), pp. 14681-14692, 2012.

[80] E. Chung, S. Yiacoumi, C. Halbert, J. Ankner, W. Wang, C. Kim and C. Tsouris, Interaction of Silica Nanoparticles with a Flat Silica Surface through Neutron Reflectometry, *Environ. Sci. Technol.*, **46** (8), pp. 4532-4538, 2012.

[81] Q. He, J. Zhang, J. Shi, Z. Zhu, L. Zhang, W. Bu, L. Guo and Y. Chen, The effect of PEGylation of mesoporous silica nanoparticles on nonspecific binding of serum proteins and cellular responses, *Biomaterials*, **31** (6), pp. 1085-1092, 2010.

[82] C. Allen, N. Dos Santos, R. Gallagher, G. N. C. Chiu, Y. Shu, W. M. Li, S. A. Johnstone, A. S. Janoff, L. D. Mayer, M. S. Webb and M. B. Bally, Controlling

the Physical Behavior and Biological Performance of Liposome Formulations through Use of Surface Grafted Poly(ethylene Glycol), *Bioscience Reports*, **22** (2), pp. 225-250, 2002.

[83] G. Storm, S. O. Belliot, T. Daemen and D. D. Lasic, Surface modification of nanoparticles to oppose uptake by the mononuclear phagocyte system, *Adv. Drug Delivery Rev.*, **17** (1), pp. 31-48, 1995.

[84] S. I. Jeon, S. H. Lee, J. D. Andrade and P. G. de Gennes, Protein-Surface Interactions in the Presensce of Polyethylene Oxide, *J. Coll. Interface Sci.*, **142** (1), pp. 149-158, 1991.

[85] A. Abuchowski, J. R. McCoy, N. C Palczuk, T. van Es and F. F. Davis, Effect of Covalent Attachment of Polyethylene Glycol on Immunogenogenicity and Circulating Life of Bovine Liver Catalase, *J. Biol. Chem.*, **252** (11), pp. 3582-3586, 1977.

[86] G. Pasut and F. M. Veronese, Polymer-drug conjugation, recent achievements and general strategies, *Polymers in Biomedical Applications*, **32** (8-9), pp. 933-961, 2007.

[87] W. I. Goldburg, Dynamic light scattering, *Am. J. Phys.*, **67** (12), pp. 1152-1160, 1999.

[88] R. Pecora, Dynamic light scattering measurement of nanometer particles in liquids, *J. Nanopart. Res.*, **2** (2), pp. 123-131, 2000.

[89] E. P. Barrett, L. G. Joyner and P. P. Halenda, The Determination of Pore Volume and Area Distributions in Porous Substances. I. Computations from Nitrogen Isotherms, *J. Am. Chem. Soc.*, **73** (1), pp. 373-380, 1951.

[90] S. Brunauer, P. H. Emmett and E. Teller, Adsorption of Gases in Multimolecular Layers, *J. Am. Chem. Soc.*, **60** (2), pp. 309-319, 1938.

[91] http://www.nbtc.cornell.edu/facilities/downloads/Zetasizer%20Manual.pdf, referred 21.5.2013.

[92] M. E. McGovern, K. M. R. Kallury and M. Thompson, Role of Solvent on the Silanization of Glass with Octadecyltrichlorosilane, *Langmuir*, **10**, pp. 3607-3614, 1994.

[93] Table of Characteristic IR Absorptions.pdf, downloaded from *http://orgchem.colorado.edu/* at 30.5.2013

[94] D. B. Mawhinney, J. A. Glass and J. T. Yates, FTIR Study of the Oxidation of Porous Silicon, *J. Phys. Chem. B*, **101** (7), pp. 1202-1206, 1997.

[95] J. -H. Park, L. Gu, G. von Maltzahn, E. Ruoslahti, S. N. Bhatia and M. Sailor, Biodegradable luminescent porous silicon nanoparticles for in vivo applications, *Nat. Mater.*, **8** (4), pp. 331-336, 2009.